VOLUME 21, 1959/60, No. 11 pp. 317-348 Published 27th September 1960

Philips Technical Review

DEALING WITH TECHNICAL PROBLEMS
RELATING TO THE PRODUCTS, PROCESSES AND INVESTIGATIONS OF
THE PHILIPS INDUSTRIES

A 75 cm RECEIVER FOR RADIO ASTRONOMY AND SOME OBSERVATIONAL RESULTS

by C. L. SEEGER *), F. L. H. M. STUMPERS and N. van HURCK.

523.164:522.6:621.396.722.029.63

The first half of the 17th century when, in rapid succession, the most outstanding discoveries in the stellar universe were made with the then newly invented telescope — the craters of the moon, the satellites of Jupiter, the phases of Venus, the stars of the galactic system, and so on — is looked on as the heroic era of astronomy. In centuries to come, the years around the middle of the 20th century may well be referred to in similar terms, for it was then that advances in radio engineering led to the construction of radio telescopes which, in their turn, brought to light unsuspected astronomical objects entirely different from those known hitherto.

Man's interest in the stellar universe dates from the earliest times. This interest led to the invention of telescopes and other optical aids with which visible radiation, and later infra-red radiation, could be observed more accurately and in greater detail. It was only about 15 years ago that astronomers realized that radio, too, could be a valuable means of widening our knowledge of the universe. In the Netherlands, for example, striking results have been obtained by radio observations at a frequency of 1420 Mc/s (wavelength 21 cm, a spectral line of hydrogen [1])). Radio observation is by no means limited to this frequency, however. On the contrary, the radio-frequency range usable for astronomical observations is very wide indeed. In the following we shall consider briefly some of the celestial objects thus brought within the purview of astronomers. We shall then describe a simple, stable and sensitive receiver for use in the frequency range from 200 to 500 Mc/s (150 to 60 cm) which has been used successfully for some years by the Netherlands Foundation for Radio Astronomy, at the Radio Observatory at Dwingeloo and elsewhere.

A principal requirement to be met by such a receiver is an extremely low inherent noise level. This is necessary in order to detect the extremely weak radiation received from most astronomical objects. The performance in this respect of the receiver referred to, though developed some years ago, ranks amongst the best that can be achieved in this field with conventional electron tubes. In latter years the parametric amplifier and the maser, too, have been developed as a means of reducing still further the inherent receiver noise contribution to the measured signal. In the coming years the parametric amplifier in particular will doubtless find wide application in radio astronomy. Its development, however, is too recent for any radio-astronomical experience to be yet available in the part of the frequency spectrum with which we are concerned.

Radio waves from outer space [2])

The spectral range covered by conventional optical astronomy comprises about two octaves

---

*) Netherlands Foundation for Radio Astronomy, Leyden Observatory. The work of this Foundation is made possible by financial support from the Netherlands Organization for the Advancement of Pure Research (Z.W.O.).

[1]) See for example C. A. Muller, A receiver for the radio waves from interstellar hydrogen, I. The investigation of the hydrogen radiation; II. Design of the receiver, Philips tech. Rev. **17**, 305-315 and 351-361, 1955/56. These articles may be referred to for a further explanation of various general facts and concepts of radio astronomy, such as the noise character of the radiation, the term antenna temperature, the directional diagram of a parabolic antenna, and so on.

[2]) A useful survey is given in the book: J. L. Pawsey and R. N. Bracewell, Radio Astronomy, Oxford Univ. Press, Oxford 1955. On equipment for radio astronomy see also: Proc. Inst. Radio Engrs., special issue, Jan. 1958.

(roughly 0.34 to 1.5 microns). The new frequency range which radio waves from outer space open up to astronomical investigations comprises some twelve octaves (*fig. 1*). At one end this range extends to millimetre wavelengths, where the radiation is absorbed by oxygen and water vapour. At the other end it extends to wavelengths of 15 or 20 metres. Longer waves are not generally passed by the ionosphere, although it has recently been shown that "windows" do occur now and then, allowing radiation of wavelengths longer than 100 metres to penetrate to the earth [3]).

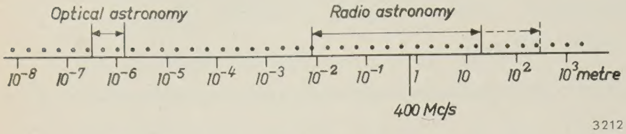

Fig. 1. Frequency spectrum of electromagnetic waves, indicating the two regions useful to the astronomer: the "optical" region (approx. 0.34 to 1.5 micron) and the radio region (approx. 8 mm to 20 m, possibly up to 300 m). The points mark divisions between octaves.

Apart from the 21 cm radiation of hydrogen, radio astronomers have found no other spectral line in the radiation received from space. Theoretically, one might expect the analogous radiation from deuterium and from the OH radical, but investigations in this direction have produced no positive results. The detectable radiation possesses, rather, a continuous spectrum.

Understandably, man's thoughts turned first to the *sun* as a possible source of radio radiation. In 1894 Sir Oliver Lodge attempted to detect such radiation, but was not successful with the means available at that time. Much later, in 1942, Hey in England found that the sun was responsible for some originally unidentifiable interference in radar. Around the same time, Southworth in America succeeded in receiving radio waves from the sun. Since then, extensive observations have been made in this field, especially in England and Australia. We can now distinguish between the background radiation of the "quiescent" sun, and the intense radiation associated with sun spots and flares. It is even possible to follow in detail the movement of such a source of radiation through the solar atmosphere. Besides the radiation from the sun, thermal radiation from the moon and from the planets Venus, Mars, Jupiter and Saturn has also been observed in the radio spectrum in recent years; this is the very long-wave part of the Planck radiation emitted by these bodies, which possesses a maximum in the infra-red. In the case of Jupiter, additional radiation is emitted at certain times, perhaps as a result of thunderstorms far more violent than any known on the earth.

Against the more or less uniform background of the radio-wave radiation received from space, sources other than the sun were discovered. The radiation from these so-called point sources, i.e. points in the heavens emitting a much stronger radiation than their surroundings, was attributed to stars, which were at first called "radio stars". At that time, however, it was not possible to identify any of these objects with any optically observed star. The "radio stars" are much "brighter" than the sun, which plays such a prominent role in relation to the earth only because of its relatively short distance from it. Such stars, as for example Cygnus A presently to be discussed, may emit radio waves whose total intensity is 10^{36} times greater than from the sun.

With the more accurate determination of position made possible by means of interferometers (see below), it later proved possible to identify a number of sources with visible objects. For example, the supernovae — stars that flare up suddenly as a result of explosion — are powerful sources of radio-wave activity. One of these is the Crab Nebula (*fig. 2*), the outburst of which was observed by Chinese astronomers in 1054. The strongest source of radio waves, Cassiopeia A, is probably also an exploded star. (It has become the practice to denote a radio-wave source according to the constellation in which it is detected, and further by a roman letter in order of discovery.)

Another identifiable and often optically visible source of continuous radio-wave radiation is the ionized hydrogen gas in the plane of our Galatic system.

This radiation originates in so-called free-free transitions. Free electrons in uniform motion cause no radiation. When such an electron approaches close to a proton, it is accelerated and this gives rise to radiation. After deflection the influence of the proton again diminishes and the electron becomes free again. The theory of these free-free transitions has been worked out by Kramers.

Radiation is also observed from other galatic systems, a familiar example of which is the Andromeda Nebula. The strong source Cygnus A has been identified with an extra-Galactic object believed to be two galaxies in collision.

The mechanism giving rise to the radiation is far from known in all cases. The radiation received from

---

[3]) G. Reber and G. R. Ellis, J. geophys. Res. **61**, 1, 1956.

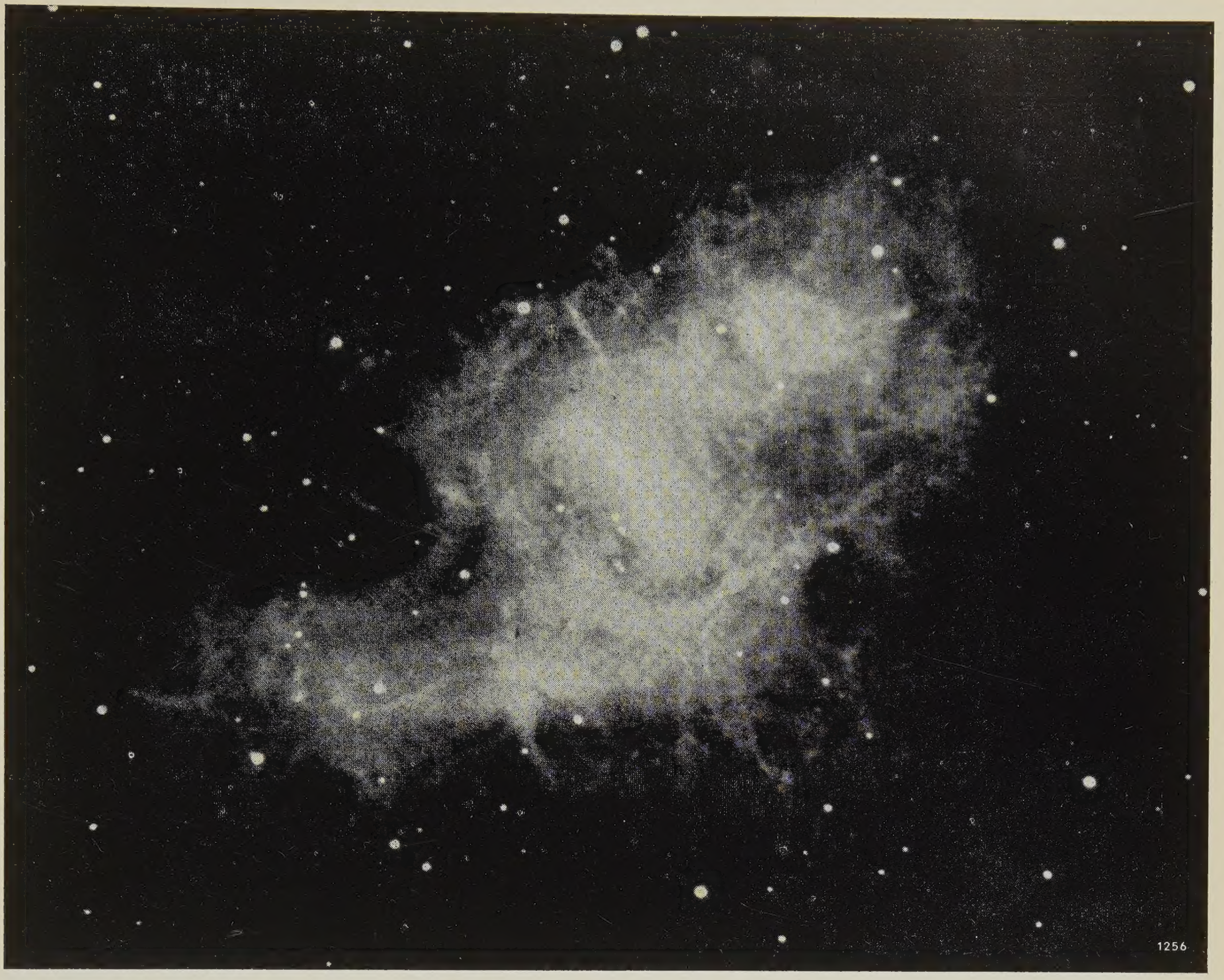

Fig. 2. The Crab Nebula, the remains of a "supernova", the outburst of which was observed by Chinese astronomers in 1054 and which has now been identified as a source of intense radio waves. One millimetre of this photograph represents 2.3 seconds of arc. The picture was taken with the 100 inch telescope in California; blue filter (0.31-0.50 μ), exposure one hour.

the Crab Nebula was found, first by optical observations and later also at radio wavelengths, to be linearly polarized. It is therefore assumed that the radiation in this case is of the synchrotron type, i.e. radiation from electrons which travel at about the speed of light in helical orbits around the lines of force of a magnetic field. It is not yet known how the electrons acquire their energy in this mechanism or how the magnetic field is created.

In order to make a conjecture as to the cause of the radio waves from a particular source, it is desirable to compare the frequency-dependence of this radiation with that following from the theoretically assumed mechanism. It is therefore necessary to carry out measurements in several parts of the spectrum. Radio astronomers, who keep in close touch with each other, try to avoid duplication of effort and choose their part of the frequency spectrum with the object of supplementing as far as possible existing data. As a result, when the 25 m radio telescope at Dwingeloo in the Netherlands came into operation, a working frequency of 400 Mc/s was selected. This choice was also influenced, of course, by the possibility of building a good receiver for this range. Moreover, the relatively high frequency of 400 Mc/s was attractive in as much as the background radiation decreases more markedly with rising frequency than the radiation from some individual sources. At 400 Mc/s these sources therefore begin to show up more clearly against the background, and this effect is enhanced because the beam width of the antenna is smaller at such higher frequencies.

Antennae for receiving the radio waves

In the observations made with our receiver the following antennae were used (see *fig. 3*):

a) a parabolic radar reflector 7.5 metres in diameter, which the Germans left behind in the Netherlands after the war; *b*) a horn antenna for calibration purposes (see below); *c*) a large parabolic reflector, 25 metres in diameter, built at Dwingeloo in the years 1954 to 1956 [4]); see *fig. 4*.

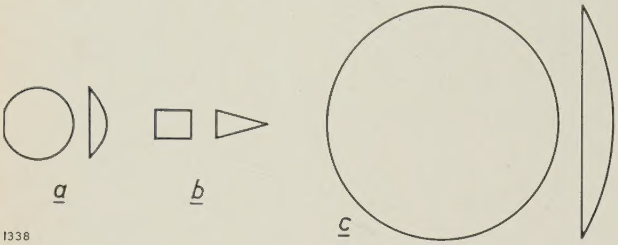

Fig. 3. Relative dimensions of the three antennae used in conjuction with the receiver described: *a*) Parabolic radar reflector of 7.5 m diameter. *b*) Horn antenna. *c*) Large, rotatable parabolic reflector of 25 m diameter, built at Dwingeloo in the years 1954 to 1956.

The main lobe of the polar diagram for the radiation received by a parabolic reflector has an aperture angle that broadly depends on the wavelength λ and the diameter d of the reflector according to the formula:

$$\varphi = 70\ \lambda/d.$$

(φ in degrees, λ and d in the same units; this aperture angle is defined such that at the angle $\frac{1}{2}\varphi$ from the lobe axis the intensity has dropped to half.) A larger reflector will thus make it possible to distinguish proportionately more detail. The 25 m reflector at 75 cm wavelength (400 Mc/s) has a lobe width of only 2.1°.

This reflector, when it came into operation in 1956, was the largest rotatable radio telescope in the world; the only larger reflector is that of the Jodrell Bank radio telescope subsequently completed at Manchester, which has a diameter of 75 metres. The observations at Dwingeloo thus showed promise of providing a relatively very accurate picture of the radio sky.

In order to make even more accurate observations than are possible with large, rotatable reflectors, antenna systems are used that function as an interferometer. Ryle in Cambridge, and Mills and Christiansen in Australia have accumulated considerable experience with such systems. The Mills arrangement comprises two mutually perpendicular horizontal rows of dipoles (cross antennae). Systems of this kind have been made in which the rows of dipoles are 500 metres long; the beam width is 0.9° at a wavelength of 3 metres. Radio astronomers in the Netherlands, in cooperation with other Western European countries, are studying a plan for a much more ambitious system in which a length of several kilometres is envisaged. A drawback of such antennae is, of course, that they cannot be directed towards every point of the sky, so that one must wait for moments when interesting points pass through the narrow beam, which is movable only to a very limited extent.

The calibration of a large antenna, i.e. the derivation of the energy flux (flux density) from the received signal presents some difficulties [5]). Since, in the case of horn antennae the received signal is much better known — theoretically and experimentally — as a function of flux density, the abovementioned horn antenna was used for the purpose of the absolute calibration discussed below.

The 75 cm receiver: general considerations

The design of a receiver is governed by the nature and strength of the signal to be received. The radiation which the astronomer wishes to receive has the character of *noise* such as is produced by thermal agitation of electrons in a resistance, or by the irregular emission of the cathode in a thermionic valve. Further, the radio astronomer must be able to deal with very weak signals. Whereas a field strength of e.g. 1 mV/m, or at least about 100 μV/m is required for a good broadcast signal, the astronomer is interested in detecting signals whose amplitude is 100,000 times smaller, corresponding to flux densities, integrated over the received spectrum, of the order of 10^{-20} W/m^2. The fact that the signals have the same character as the inherent noise of the receiver is an added difficulty. The inherent noise in a normal receiver may correspond to an input-resistance temperature of several hundreds or thousands of °K. Against this background it is required to detect signals corresponding to a temperature increment of about 1° due to a cosmic source. For this reason it is of paramount importance to reduce the inherent noise of the receiver to the minimum, and moreover to keep the gain of the

---

[4]) The radio telescope, Dwingeloo; six articles (in Dutch) by H. C. van de Hulst; B. G. Hooghoudt; R. J. Schor; W. Huisman; B. B. Schierbeek; G. H. Jöbsis; De Ingenieur **69**, O1-O19, 1957.

[5]) The flux density, expressed in watt/m^2 per c/s, is the energy incident per second and per unit bandwidth on a surface area of one square metre of the antenna. Where the source is extensive the concept "brightness" may also be introduced; this is the flux density divided by the solid angle subtended by the source at the point of observation.

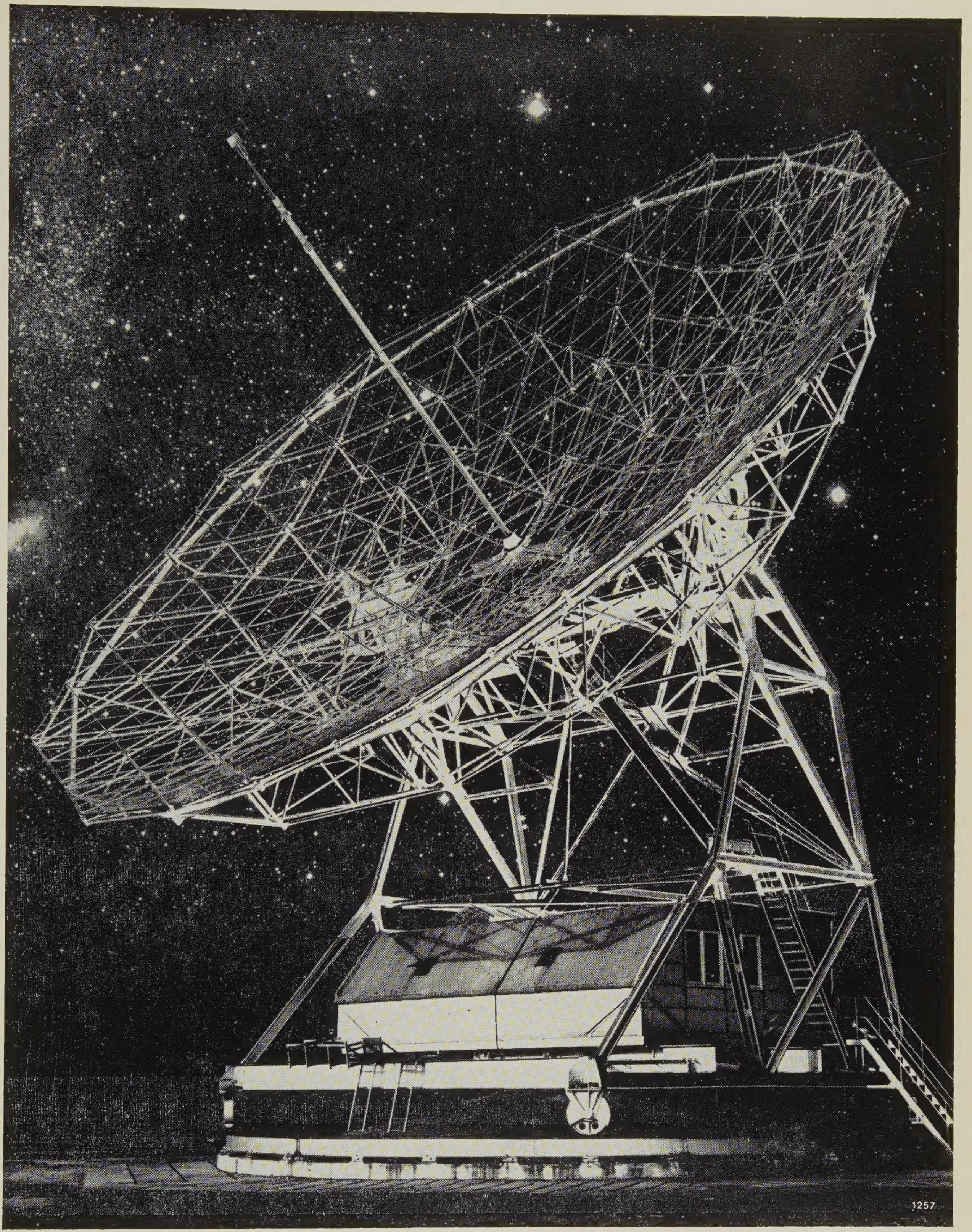

Photo-montage by H. Kleibrink

Fig. 4. The 25 m parabolic reflector of the radio telescope at Dwingeloo.

receiver extremely constant whilst scanning the sky.

The following considerations indicate the most important fundamental limits to the reduction of the inherent noise level. After amplification, the signal is detected. The output power I of the detector fluctuates, even though the input noise signal and the gain are constant. The magnitude of the fluctuation is given by

$$\overline{(I - I_0)^2} = \frac{pI_0^2}{\tau \Delta f}, \quad . \; . \; . \; . \quad (1)$$

where I_0 is the mean output power, τ the time constant and Δf the bandwidth of the receiver, and p a constant of the order of magnitude of unity, which depends to some extent on the frequency response of the receiver and on the detector characteristic. A signal, in order to be observed, must have an amplitude of at least the order of magnitude of these fluctuations.

The fluctuation, a measure of which is $\sqrt{\overline{(I-I_0)^2}}$, is evidently proportional to the noise level I_0. Further, the variation of a fluctuating quantity is inversely proportional to the root of the number of independent "readings" of this quantity; this accounts for the factor $\tau\Delta f$ in the denominator.

From eq. (1) it might be thought that, by increasing the time constant τ and the bandwidth Δf, one could arbitrarily reduce the lower limit of the measurable signals. The situation is not as simple as that, however. As the bandwidth increases the contribution of the inherent noise of the receiver increases more strongly than that of the detected signal, owing to the quadratic frequency-dependence of the noise factor (see below). Moreover, there is a greater chance of receiving an interference signal. Increasing the time constant also meets with difficulties. The time needed for a single measurement then becomes longer, and if the sky is continuously scanned the antenna must be made to move more slowly [6]). This is most undesirable for observations that extend over weeks or months, such as those involved in the accurate charting of regions of the sky. Again, with a larger time-constant value it is less easy to ascertain whether perhaps an interference peak has occurred that would vitiate the result of measurement. The choice of bandwidth and time constant must therefore be a compromise. The present receiver can have an optional bandwidth of 10 or 1 Mc/s, and the time constant can be varied, according to circumstances, from 0.1 to 10 sec. For some purposes the observation time can be lengthened by keeping the antenna directed for a certain time towards the same point and by averaging the recorded intensity. This has the same effect as a very large time constant, but one can now see from the recording whether an interference peak has occurred.

Before going into details of the receiver we shall discuss briefly the way in which the inherent noise of a receiver is determined.

The noise factor and its measurement

The inherent noise which a receiver contributes to the noise level is expressed by the noise factor, F. This factor indicates by how many times the noise power at the output terminals is greater than that of of an ideal receiver (which itself contributes no noise) when no noise source is present other than the normal input impedance, at a standard temperature T_0. As this impedance we can take, for example, the characteristic impedance of the connection cable on which the receiver normally operates, namely 50 ohms. The noise power delivered by an impedance is proportional to its temperature T. We might also say, therefore, that owing to the noise contribution of the receiver the input impedance has an apparent temperature $F \times T_0$. The receiver noise thus gives rise to an apparent temperature increase of $(F - 1)T_0$.

This leads directly to one of the methods of measuring the noise factor [7]). The output noise power P_1 is measured with the input impedance at a temperature T_1, and the measurement is repeated at a different temperature T_2, giving the noise power P_2. We may then write:

$$P_1 = a\{(T_1 + (F{-}1)T_0)\}, \quad . \; . \; . \quad (2a)$$

$$P_2 = a\{(T_2 + (F{-}1)T_0)\}. \quad . \; . \; . \quad (2b)$$

In accordance with the IRE Standards [8]) the standard temperature T_0 is taken to be 290 °K. a is a constant proportional to the receiver gain. We eliminate a from (2a) and (2b), and the result is:

$$F{-}1 = \frac{P_1T_2 - P_2T_1}{(P_2 - P_1)T_0}. \quad . \; . \; . \; . \quad (3)$$

A practical procedure is first to take a measurement with a resistance of 50 ohms at room temperature connected at the receiver input, and then with a resistance whose value is 50 ohms at the temperature of liquid nitrogen (77.5 °K). The deflection of the detector is previously calibrated in terms of delivered power, by a method which will be touched on later.

Once the noise factor of the receiver has been determined, one can conversely derive from the measured output signal the temperature of the input impedance. This applies not only to a true resistance but also to the radiation resistance of the antenna. The "antenna temperature" is, subject to certain conditions, equal to the temperature of the space upon which the antenna is directed, or, since the temperature of that space may differ from place to place, equal to the average temperature of the space seen by the antenna. (Each region is given a weighting factor corresponding to the size of its solid angle and its direction in the antenna polar diagram: the average temperature is thus a "weighted mean".) Frequently this is virtually the equivalent temperature of the radiation in the main direction of the antenna. The variation of this temperature over the sky, which is a measure of the radiation intensity, is what the radio-astronomer seeks to measure.

---

[6]) Compare the entirely analogous problem of the continuous recording of an X-ray diffraction diagram: Philips tech. Rev. 17, p. 208 *et seq.*, 1955/56.

[7]) Various methods of determining the noise factor are discussed in N. van Hurck and F. L. H. M. Stumpers, An automatic noise-figure indicator, Philips tech. Rev. **18**, 141-144, 1956/57.

[8]) IRE Standards on electron tubes: Definitions of terms, Proc. Inst. Radio Engrs. **45**, 983-1009, 1957.

Details of the receiver

The receiver is essentially a normal superheterodyne type, having an intermediate frequency of 50 Mc/s. A silicon-crystal diode serves as the mixer stage. The block diagram of the whole receiver is shown in *fig. 5*. We shall now deal successively with some particular features, namely the high-frequency amplifier, measures to stabilize the amplification, and the detector.

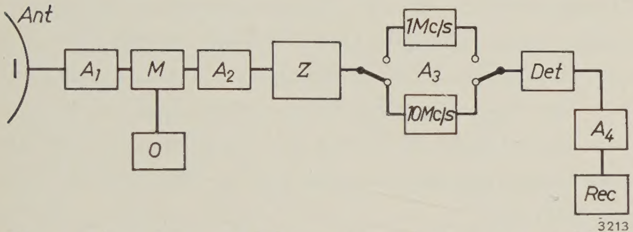

Fig. 5. Block diagram of the receiver. *Ant* antenna. A_1 hign-frequency amplifier. *O* local oscillator. *M* mixer (silicon diode). A_2 intermediate-frequency preamplifier. *A* calibrated attenuator, adjustable in steps of 1 dB (see section on calibration). A_3 intermediate-frequency amplifiers with two optional bandwidths. *Det* detector. A_4 DC amplifier with variable time constant. *Rec* recording instrument.

The high-frequency amplifier

The most suitable circuit for the high-frequency amplifier is the cascode circuit [9], which combines a low noise factor with high gain and great stability (no tendency to oscillation). In this circuit the cathode of an amplifying valve, whose grid is earthed, is connected for high frequencies to the anode of the preceding valve. For the frequency range in question the best valve in both places in the circuit is the type EC 57 disc-seal triode, which has the advantages of extremely short and constant electron-transit times and the high fraction of the saturation emission from an L-cathode that can be usefully employed [10]. The gain of two type EC 57 valves in cascode is about 36 dB at 400 Mc/s. A result of this high gain is that the following stage, the mixer, makes only a minor contribution to the noise factor.

The noise factor of a multi-stage amplifier is given by:

$$F = F_1 + \frac{F_2-1}{G_1} + \frac{F_3-1}{G_1G_2} + \dots + \frac{F_k-1}{G_1G_2\dots G_{k-1}} + \dots, \quad (4)$$

where F_k is the noise factor of the k^{th} stage alone, and G_k the available power gain of that stage. It is assumed here that the F and G values do not depend significantly on frequency within the bandwidth of the receiver.

The high-frequency amplifier is shown in more detail in *fig. 6*. The antenna signal is applied via a 50 ohm coaxial cable to the amplifier input. Here an impedance transformer [11] (T_1) enables the input impedance of the first valve (B_1), on which the noise factor is highly dependent, to be adjusted to the optimum value. The signal now arrives on the grid of the first valve, whose cathode is earthed for high frequencies. The cathode of the second valve is connected with the anode of the first. The stray capacitance of this point with respect to earth, which would form a short-circuit to the high-frequency anode current of the first valve, is effectively neutralized by tuning with a lecher system, T_2. (The two inner conductors in T_2 which are shown in fig. 6, together constitute for this purpose a single conductor, being interconnected at their ends. The arrangement in the same form as the impedance transformer T_1 is chosen here only because it facilitates the conduction of the necessary direct voltages to the valve electrodes — which must not of course be thereby short-circuited for high frequencies.) Similarly, the anode-grid capacitance of the first valve is neutralized by means of a simple coil, L, tunable with a sliding core. (The core is made of silver-plated bronze to limit eddy-current losses.) This is a variant of the familiar neutrodyne system, but its purpose is not to prevent instability due to feedback, the voltage gain of the first valve being too small (equal to unity) to produce such an effect.

---

[9] Introduced and analysed by H. Wallman, A. B. MacNee and C. P. Gadsden, A low-noise amplifier, Proc. Inst. Radio Engrs. **36**, 700-708, 1948.

[10] G. Diemer, K. Rodenhuis and J. G. van Wijngaarden, The EC 57, a disc-seal microwave triode with L cathode, Philips tech. Rev. **18**, 317-324, 1956/57. The EC 57 valve used in our receiver has since been superseded by type EC 157, having a cathode of longer life. A general discussion of triode noise at high frequencies is given by G. Diemer and K. S. Knol, Philips tech. Rev. **14**, p. 236, 1952/53.

[11] K. S. Knol and J. M. van Hofweegen, A universal adjustable transformer for U.H.F. work, Philips Res. Repts. **3**, 140-155, 1948.

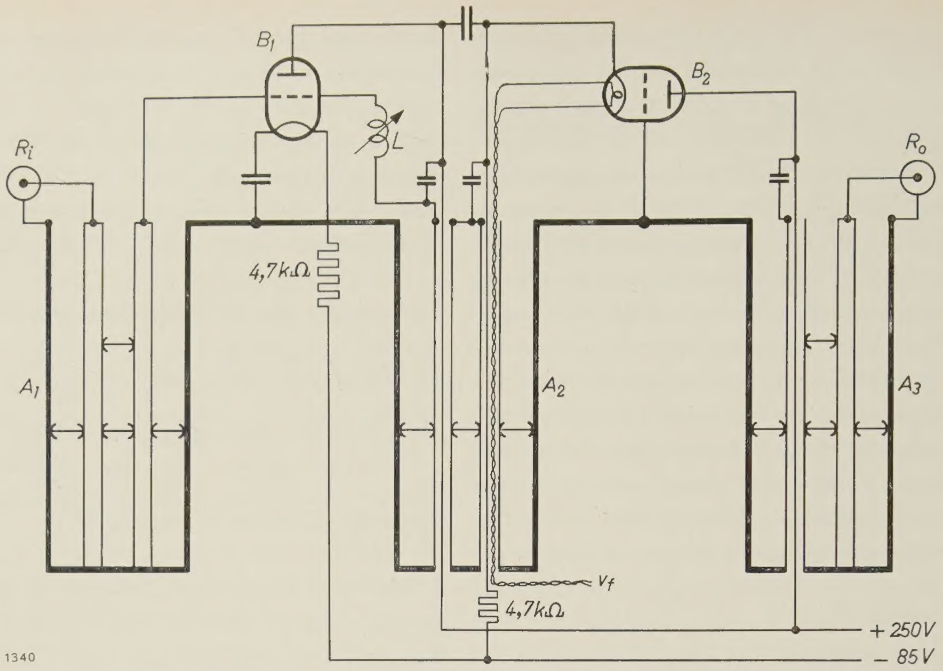

Fig. 6. Diagram of high-frequency amplifier. B_1 and B_2 two disc-seal triodes type EC 57. R_i coaxial cable of 50 ohms characteristic impedance, serving as input resistance. T_1 matching transformer in the form of a lecher system with two sliding shorting discs. T_2 lecher system for tuning the stray capacitance between the cathode of B_2 and earth; for convenience the same type is used as for T_1. L coil with plunger core for neutralization. T_3 matching transformer for a 50 ohm cable R_0, which functions as output resistance. The cathode of both valves receives a negative bias via a resistance of 4.7 kΩ; this bias determines the anode current (20 mA).

The object of the neutralization, in conjunction with the tuning of T_2, is rather to give the second valve a high input impedance, which, as experiments have shown, is needed to keep down the noise contribution of the valve. In the anode circuit of the second valve another impedance transformer (T_3 in fig. 6) ensures correct matching to the 50 ohm cable which conducts the signal to the mixer.

The arrangement of two triodes in cascode constitutes a system possessing the favourable properties of a pentode, but without the drawback of partition noise which attaches to the pentode. Whereas in the pentode the screen grid limits the coupling between input and output circuit (and thereby suppresses the tendency to oscillation) this is done in the cascode by the grid of the second triode, in which there is no current partition. Compared with a circuit having a single triode in the earthed grid configuration. the cascode arrangement possesses the advantage, typical of a pentode, of a much higher gain: the high cathode impedance which would be required for single triode to give a small noise factor, gives rise to negative feedback effects, which are of course not conducive to a high gain.

The noise factor found, using a selected EC 57 for the first valve, is plotted in *fig.* 7 as a function of the tuning frequency. At 400 Mc/s the noise factor F was 2.5. Measurements on some thirty valves yielded an average value at this frequency of $F = 2.9$, with a spread of $\pm$ 0.3. The temperature $(F - 1)T_0$, also shown in the figure, corresponds to the background, referred to above, against which an extra-terrestrial signal must stand out. The temperature corresponding to the above-mentioned noise factor $F = 2.5$ is $(F - 1)T_0 = 435$ °K. With the aid of equation (1) we therefore find that, at a bandwidth of 10^7 c/s and a time constant of 10 sec, it is possible to detect an antenna temperature increment of $\sqrt{435^2/(10 \times 10^7)} \approx 0.05$ °K.

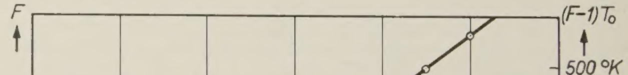

Fig. 7. Noise factor F of the receiver, measured on a selected EC 57 valve used as the first high-frequency amplifier (B_1 in fig. 6; this tube determines practically the entire inherent noise of the receiver, of which F is a measure). The graph is a plot of $F{-}1$ versus the tuned frequency f in Mc/s. At 400 Mc/s the value of F is 2.5. The points lie to a good approximation on the straight line defined by the equation: $F - 1 = 0.377 \times f/100$. On the right is a scale in terms of $(F{-}1)T_0$, i.e. the antenna temperature, equivalent to the inherent noise of the receiver.

The lower limit of the frequency range in which the receiver can operate is determined by the limited length (0.50 m) of the lecher systems used: tuning is not possible below about 200 Mc/s. The upper limit of the frequency range is determined by the neutralization: the simple method employed works well up to more than 500 Mc/s. With more elaborate devices it would probably be possible to reach 700 or 800 Mc/s.

Tuning with the lecher systems is so sharp that the incoming signal having the image frequency — which, due to frequency-changing in the mixing stage, also comes within the I.F. band — is attenuated by 45 dB with respect to the required signal.

The high-frequency amplifier is aligned by first setting all variables at maximum gain by means of a signal generator. Next, the first stage is adjusted for minimum noise factor by varying the impedance transformer T_1, the neutrodyne circuit and the tuning of the first anode (T_2). The automatic noise-figure indicator, described earlier in this journal [7], is well-nigh indispensable for this purpose, since it shows immediately the effect of each change. Without it, a rather cumbersome procedure is necessary.

Special measures to ensure stability

We have seen that the amplifier must be very stable if spurious variations in the gain are not to be regarded as changes in the received noise power. Mains-voltage fluctuations are dealt with by a voltage stabilizer, which reduces a ± 10 % variation to a change of less than 0.1% in the supply voltage. The direct voltages for the valves obtained from this stabilized supply are held constant to within 1 in 10^5 with the aid of a stabilizer using a standard cell as reference. All amplifier stages are fitted with high cathode resistances, thus firmly establishing the bias of the valves, and also resulting in satisfactorily stable high-frequency characteristics. The detector used has the special feature that the level to be measured has no effect on the bandwidth and gain of the preceding amplifier valve (see below). Furthermore, the ambient temperature is kept as constant as possible in order to avoid temperature effects.

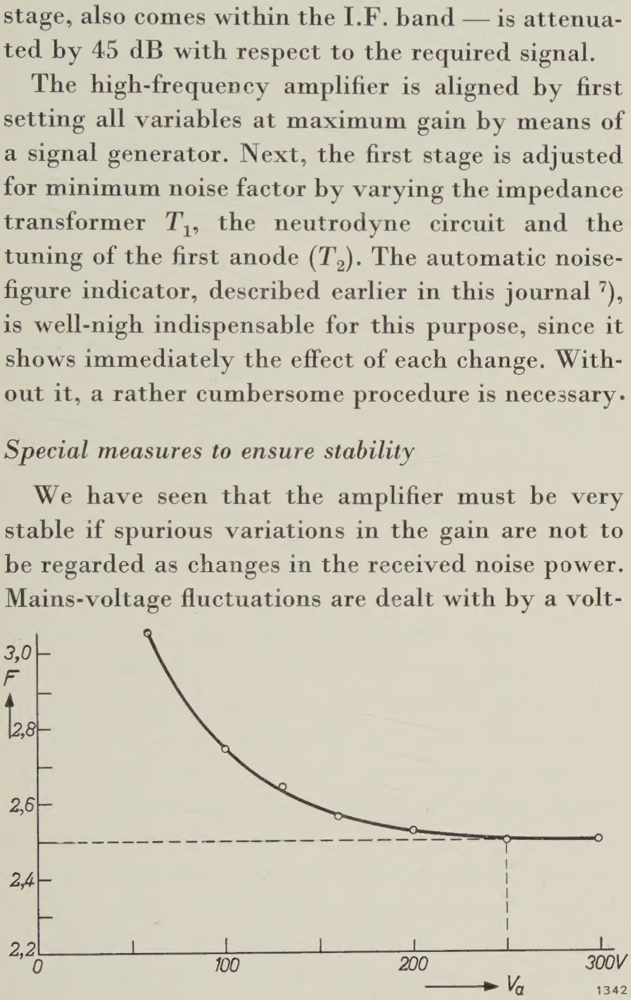

Fig. 8. Variation of the noise factor as a function of the direct anode voltage V_a on B_1. When V_a is varied, hardly any change is required in the adjustment of T_2 (see fig. 6). The value chosen was V_a = 250 V.

Special care is devoted to the aligning of the high-frequency amplifier. After adjustment for minimum noise factor, a test is made to ascertain to what extent the noise factor still depends on the biasing voltages. When the anode voltage of an EC 57 triode is gradually raised, the noise factor drops sharply between 60 and 160 volts; at higher voltages the effect is slight (*fig. 8*). An anode voltage of 250 V was considered sufficient for a favourable noise factor. Next, the variation of the noise factor as a function of the anode current was measured at 250 V (*fig. 9*). The minimum, which lies at 20 mA, was found to be fairly flat, which means that anode-current variations have little effect. It might now be asked whether, at this setting, the noise factor depends to any marked extent on the filament voltage. *Fig. 10* shows that this is not the case.

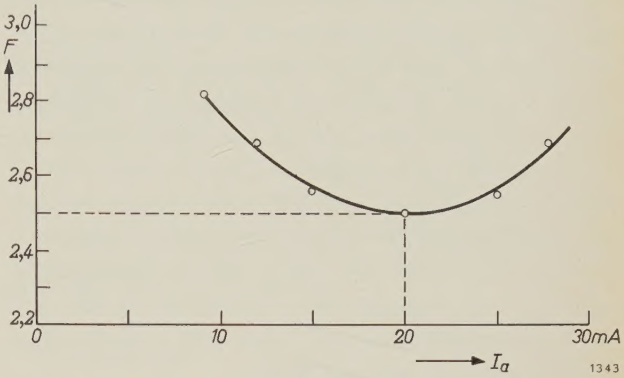

Fig. 9. Variation of the noise factor as a function of the anode current I_a. The optimum setting was found to be I_a = 20 mA; however, the minimum is rather flat.

It was mentioned above that the bandwidth of the receiver, which is normally 10 Mc/s, can be reduced to 1 Mc/s (viz. by switching-in an additional

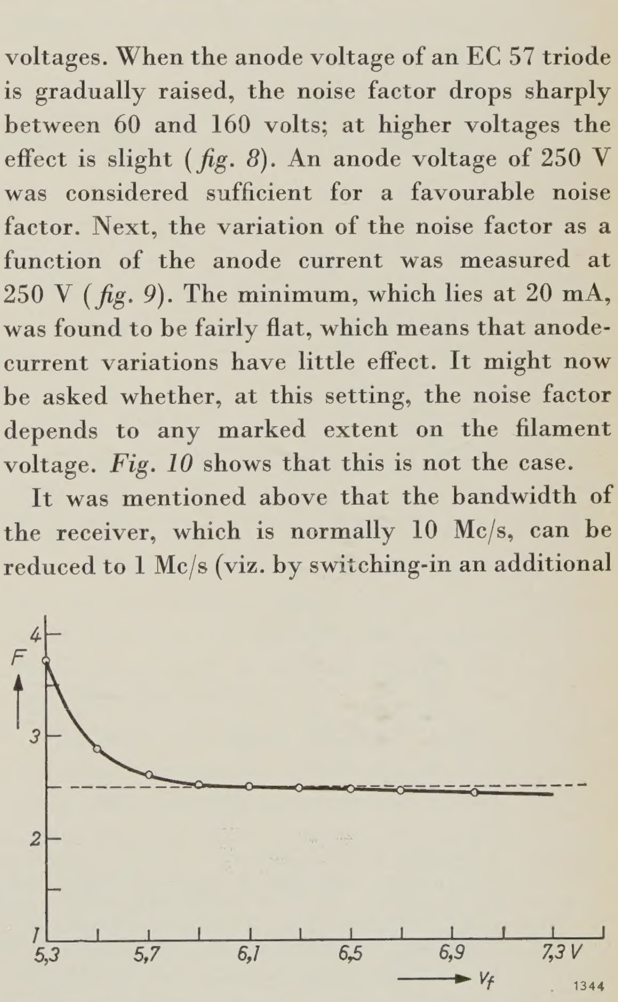

Fig. 10. Variation of noise factor as a function of valve heater voltage v_f.

band filter, see fig. 5) if interference makes it necessary. One might expect the noise factor at a bandwidth of 1 Mc/s to be appreciably smaller than at 10 Mc/s, considering that the noise factor rises quadratically with increasing (positive or negative) deviation from the tuning frequency [9]). However, the minimum to which the receiver is tuned is very flat, so that the noise factor variation for a frequency deviation of 5 Mc/s is of no significance.

Although the receiver is in fact suitable for the frequency range from 200 to 500 Mc/s, for the radio-astronomical observations to be described it has been operated solely at the fixed frequency of 400 Mc/s. This enables the frequency of the local oscillator to be stabilized with a quartz crystal. The crystal vibrates at a frequency of 29.17 Mc/s; this is trebled and twice doubled to obtain the required frequency of 350 Mc/s. For the latter frequency-doubling, where a fairly high power is demanded at the high frequency of 350 Mc/s, use is made of a small transmitting valve, type QQE 02/5.

The measures described resulted in a very stable receiver.

A known method of reducing the effect of gain fluctuations still further is to switch continuously between a reference noise source and the source to be measured (see [1])). Unless two receivers are used, however, this means losing half the observation time, This complication was therefore avoided here.

The detector

In the design of the receiver, it was endeavoured to maintain complete linearity up to the detector over a very wide range of signal amplitudes. Non-linear distortion of the noise signal, owing to the clipping of the peaks, for example, would cause errors in the intensity values. For this reason a constant-impedance type detector was chosen [12]) (*fig. 11*) so that, as opposed to normal diode detection, the last stage of the I.F. amplifier is not subjected to a varying load when the signal amplitude varies. For the same reason, instead of the 1.5 W valve conventionally used in wide-band amplifiers, a type E 81 L valve is fitted in the last I.F. stage, which has a power of 6.5 watt and delivers a sinusoidal output voltage up to 30 V without significant distortion. True, the r.m.s. value of the signal applied to the detector amounts to no more than 3 V from the most powerful astronomical objects. Owing to the noise character of the signal, however, much higher instantaneous values appear at the output of the I.F. amplifier: the amplitude 12 V occurs, for example, during 0.01% of the time.

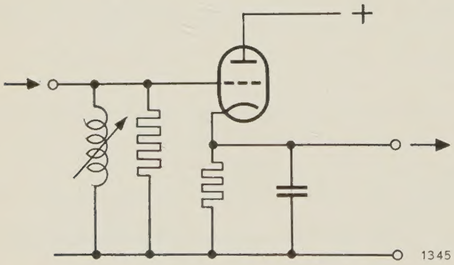

Fig. 11. Diagram of the detector (constant-impedance type). Owing to the presence of the *RC* network the anode current is a measure of the average amplitude over several cycles of the signal voltage applied to the grid (anode detection). Since hardly any grid current flows, the preceding stage is not loaded and the gain linearity is maintained up to peak voltages of e.g. 30 V.

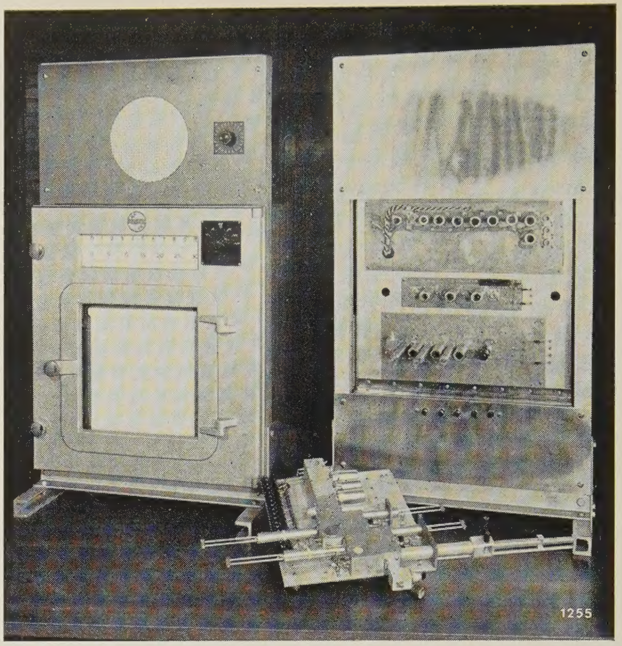

Fig. 12. The complete receiver. The chassis in the foreground contains the high-frequency amplifier (somewhat differently constructed but essentially the same as described in the text), the mixer diode and the IF preamplifier. This assembly is mounted at the pole of the parabolic reflector (fig. 4), where the mast is fixed, the other end of which carries, in the focal point of the reflector, the antenna proper (a kind of horn) and through which the coaxial connecting cable passes. The panel on the right contains the power-supplies, the detector and D.C. amplifier and the two I.F. amplifiers (for 10 and 1 Mc/s, respectively), On the left, the recording instrument and the monitoring loudspeaker.

The detector voltage is fed to the recording meter via a DC amplifier, which is stabilized by negative feedback and by periodic switching to a reference signal [13]). This amplifier serves not only to produce a low output resistance, for matching to the recording instrument, but also enables the zero point of the scale to be placed far outside the reading range of the meter or strip recorder: the signal variations can thus be recorded enlarged up to 100 times. Furthermore, it is a simple matter to make the time constant of the DC amplifier variable. In this way the time constant of our receiver was made variable, as mentioned above, between 0.1 and 10 sec.

---

[12]) W. K. Squires and R. A. Goundry, Electronics **25**, April 1952, p. 109.

[13]) S. Landsberg, A general-purpose drift-free D.C. amplifier, Philips Res. Repts. **11**, 161-171, 1956.

A photograph of the complete receiver appears in *fig. 12*.

Calibration of the receiver

The calibration of the receiver comprises a number of somewhat diverse procedures: measuring the noise factor of the receiver, determining the detector "law" (i.e. the relation between the output voltage of the detector and the noise power applied as signal to the receiver input) and calibrating the antenna.

Measuring the noise factor

The principle of measuring the noise factor having been described above, we shall deal here at greater length with a single, and rather unusual, detail of the set-up. For the measurement it is necessary to connect to the input a resistance of 50 Ω, which must first be held at room temperature and subsequently at the temperature of liquid nitrogen. A pure resistance, without inductance or capacitance, at a frequency of 400 Mc/s is feasible only as a coaxial resistance. However, not every coaxial resistance can tolerate immersion in liquid nitrogen. After each cycle of cooling and re-heating, such resistances do not usually return to exactly the same resistance value. A coaxial resistance that gives reproducible results under these conditions was constructed as follows. A ceramic rod is coated at one end with a thin layer of metal of length about 15 mm. This has a resistance of 50 Ω. The metal layer is a mixture of gold and platinum, prepared from a suspension marketed under the name "Zilverglans" (Regout, Maastricht). This preparation is applied with a brush and subsequently baked-in. The rest of the ceramic rod is then given a coating of silver making contact with the metallized end. It now constitutes the inner conductor of a coaxial system, the rest of which is formed by the coaxial cable to the receiver. The outer conductor is formed by a copper tube, dimensioned so as to obtain a characteristic impedance of 50 Ω. At the position of the resistance layer the outer conductor is tapered (*fig. 13*) and at the end, at a, the inner and outer conductors are soldered together. The tapering provides at each point, as it were, a match to the still remaining portion of the ohmic resistance.

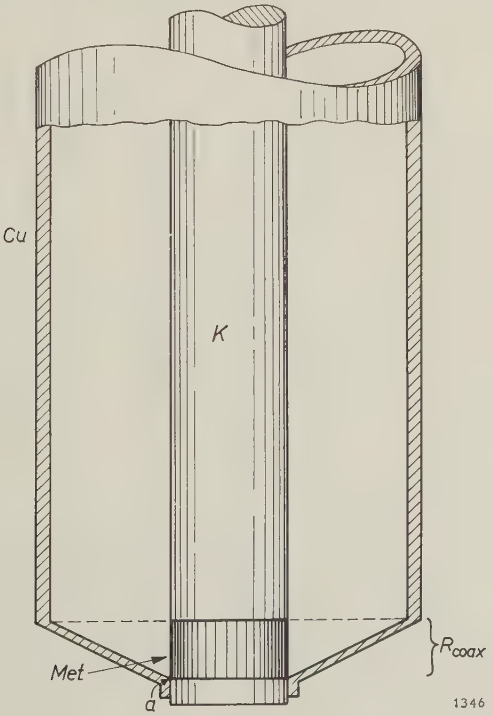

Fig. 13. Construction of the coaxial resistance, R_{coax}, designed for immersion in liquid nitrogen. *Cu* copper outer conductor. *K* silver-plated ceramic rod, coated at one end with a special metal layer *Met*.

The equivalence of the cooled resistance with a similar coaxial resistance held at room temperature is checked with an admittance bridge. If a small difference exists, the resistance at room temperature can be made exactly equal to the other by means of an impedance transformer [11]), like that described above under the sub-heading *High-frequency amplifier*. (This transformation is applied to the resistance at room temperature because losses occurring during this process must be regarded as contributions to the total resistance, due to resistances at room temperature.)

The detector law

For determining the detector law — which must be known in order to be able to measure the noise factor — a calibrated attenuator is incorporated in the I.F. amplifier; see fig. 5. This is a wide-band attenuator, with a 50 Ω termination at both ends. It contains five stages, giving an attenuation of 1-2-3-4-10 dB, respectively, and is operated by push-buttons; in this way an attenuation up to 20 dB can be introduced in steps of 1 dB. The attenuator was tested at the Naval Research Laboratory in Washington, D.C.; the deviation from the nominal attenuation was found in no case to be greater than 0.1 dB.

With no input voltage, i.e. solely as a result of the inherent noise of the receiver, the detector at a particular setting of the apparatus delivered a D.C. output of 0.966 V, with the attenuator set at 0 dB. If we now switch in 1 dB attenuation and apply a noise signal of sufficient strength to produce the same meter deflection, we find that, on returning to an attenuation of 0 dB, the D.C. output is 1.173. Proceeding along these lines we obtain the data presented in *Table I*.

The steps of 1 dB are obviously much too coarse for radio-astronomical observations. We can interpolate with the following formula derived from the table:

$$1000\,E = 950 + 202\,a + 13\,a^2 + a^3 \;.\;.\;. \quad (5)$$

The individual values of E in the table show small irregular deviations x from this formula. These are attributable to reading errors in E or to errors in the attenuator (errors as small as 0.03 dB are sufficient

Table I. The detector law determined by means of the calibrated attenuator: direct voltage output E as a function of input noise power a.

Applied input noise power a dB	Equiv. temperature of input resistance °K	D.C. voltage E at output V	Deviation x from eq. (5) mV	Graphic interpolation of x
0	290	0.966	+ 16	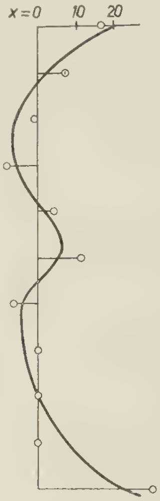
1	365	1.173	+ 7	
2	460	1.413	— 1	
3	579	1.692	— 8	
4	728	2.034	+ 4	
5	917	2.421	+ 11	
6	1155	2.84	— 6	
7	1452	3.34	0	
8	1830	3.91	0	
9	2310	4.55	0	
10	2900	5.30	+ 30	

to explain the discrepancies). In practice a correction is applied to the values interpolated in accordance with (5); this correction is obtained by graphic interpolation of the x value (see graph in the table).

Calibration of the antenna

With the aid of the detector law the measured radiation intensities are expressed in relation to a fixed datum level, the inherent noise of the receiver. To determine the absolute radiation intensities, the primary unknown factor being the radiation-receiving power of the antenna, it is sufficient to know accurately the absolute value of the flux density of a single radio star. This antenna "calibration" is necessary in order to be able to compare the results of different radio observatories, and particularly in order to combine measurements at different wavelengths into a reliable spectral distribution. As mentioned in the introduction, this is important for the purpose of testing theoretical predictions regarding the mechanism of the radiation.

The "calibration star" chosen was the radio-source Cassiopeia A already referred to. Apart from the short waves, where the sun has the greatest intensity, this star is the most powerful source of extra-terrestrial radio waves in the whole radio spectrum.

The calibration was carried out in several steps, using the horn antenna mentioned earlier. The dimensions of this antenna were: axial length 5.625 m (= 7.500 λ), vertical aperture 3.028 m (= 4.038 λ) and horizontal aperture 3.756 m (= 5.008 λ). From these dimensions a gain of 20.95 dB is calculated with respect to the isotropic antenna [14]). The gain factor of the 7.5 m reflector was then determined by taking alternate measurements on a single source (viz. the sun) with this reflector and with the horn antenna; the gain found was 27.1 dB. The flux density of Cassiopeia A was now measured with a simple interferometer arrangement, using both antennae placed at a distance of 20 λ apart. With this arrangement the beam of the radiation received is so narrow as to neutralize the more continuously distributed background radiation, and the gain factor of the whole is known from the preceding steps. The result obtained was a flux density of 56.2×10^{-24} W/m^2 per c/s, corresponding to an antenna temperature of about 800 °K. (A detailed description of this measurement is given in the article in B.A.N. No. 472, referred to under [15])).

During the operation of the receiver installation the antenna is directed towards Cassiopeia A at regular intervals of, say, an hour, to check the amplification of the receiver. The receiver has proved to be so stable that no adjustment is required for weeks on end.

Some radio-astronomical observations made with the receiver described

As mentioned in the introduction, the Netherlands Foundation for Radio Astronomy have had the receiver described in operation for some years, mostly at Dwingeloo. During this time the receiver has given no difficulties whatsoever. Some results obtained in conjunction with the Observatory of Leiden University [15]) are briefly mentioned below.

An observation was made with the aid of the 7.5 m reflector of the partial eclipse of the sun on 30th June 1954. Owing to severe interference from a neighbouring transmitter the bandwidth had to be limited to 1 Mc/s (to be more exact: 0.9 Mc/s) and a time constant of only 0.1 sec was used in the detector in order to distinguish more clearly the effect of disturbances, originating for example from car ignition systems. Observation began two hours before the eclipse and was continued for one hour afterwards. The reflector did not follow the sun automatically, but was adjusted at two-minute intervals. *Fig. 14* shows a comparison of the observed eclipse with that calculated geometrically. A smooth curve can be drawn through the measured points with an error within one scale unit, except at the beginning and the end, where the error may be $1\frac{1}{2}$ scale units. During this eclipse the sun was very calm. The average radio-brightness of the sun at 400 Mc/s, calculated for a diameter of about 30 minutes of arc, corresponded to that of a black body having a temperature of 6 × 10^5 °K. The reference level for this measurement was a resistance at room temperature, which was switched-in at least once every ten minutes.

---

[14]) S. A. Schelkunoff and H. T. Friis, Antenna theory and practice, Wiley, New York 1952.

[15]) C. L. Seeger, 400 Mc/s partial eclipse observations on 30 June 1954, Bull. Astron. Inst. Netherlands (B.A.N.) No. 461, 3 Dec. 1955, 273-283.
C. L. Seeger, G. Westerhout and H. C. van de Hulst, The flux densities of some radio sources at 400 Mc/s, B.A.N. No. 472, 26 Nov. 1956, 89-99.
C. L. Seeger, A tentative measure of the flux density of Cassiopeia A at 400 Mc/s, B.A.N. No. 472, 26 Nov. 1956, 100-104.
C. L. Seeger and G. Westerhout, Observations of occultations of the Crab Nebula by the moon at 400 Mc/s, B.A.N. No. 478, 9 Sept. 1957, 312-316.
C. L. Seeger, G. Westerhout, T. Hoekema and R. G. Conway, shortly to be published in B.A.N.

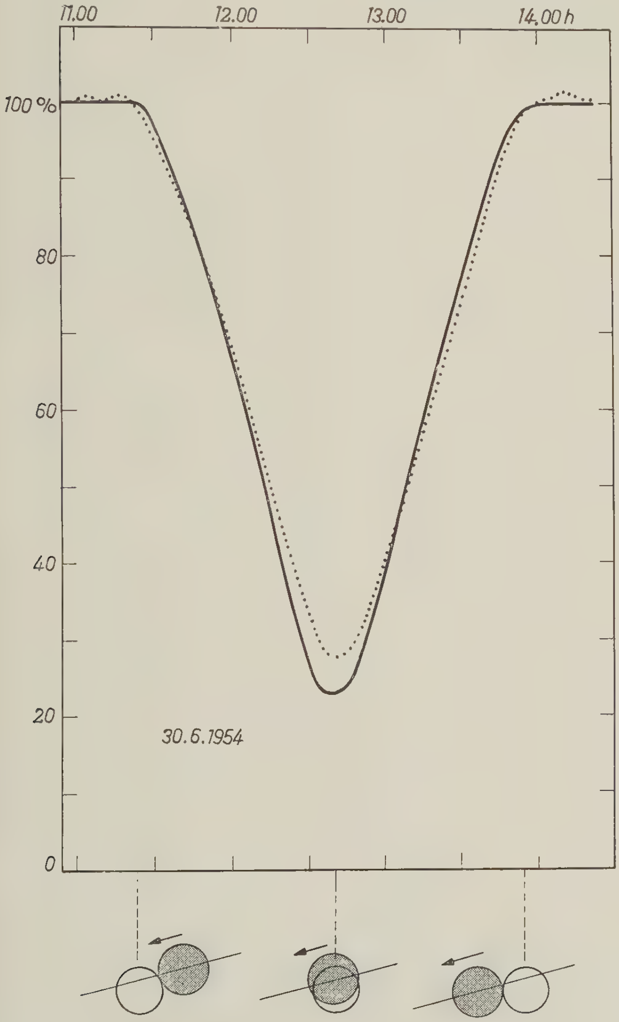

Fig. 14. Relative change of solar radiation at 400 Mc/s (arbitrary units), measured during the partial eclipse of the sun on 30th June 1954 at Waalsdorp (dotted curve). The solid curve is the geometrically calculated curve of the eclipse (percentage size of the visible surface of the sun). The position of the moon in relation to the sun at the beginning, zenith and end of the eclipse are illustrated below. Comparison of the measured and calculated radiation intensities shows that the radio "brightness" of the sun is not entirely constant over its surface (see the first article quoted under footnote [15]).

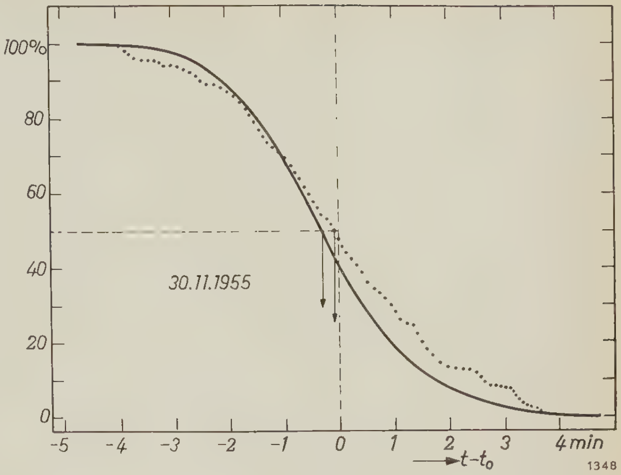

Fig. 15. Intensity of the 400 Mc/s radiation from the radio source *Taurus A* (the Crab Nebula, see fig. 2) recorded at Dwingeloo during the first part of the occultation by the moon on 30th November 1955 (dotted curve). The solid curve is the optically observed curve of the eclipse. t_0 is the calculated time at which the middle of the twin star, near the centre of the Nebula, disappeared behind the moon. The observation showed that the radio centre of the Crab Nebula differs only by about 12 seconds of arc from the optical centre point (in green light).

Another event observed with this receiver was the occultation of the Crab Nebula by the moon on 3rd and 30th November 1955. The large radio telescope at Dwingeloo was not entirely ready at that time and was unable to follow the occultation automatically. Since the event would not recur in our latitude for many years, the construction work was interrupted for four days in order to make the observation. The recording (*fig. 15*) showed that the radio centre of the Crab Nebula (Taurus A) virtually coincides with the optical centre. Broadly speaking, the angular extent of the Nebula at 400 Mc/s is the same as that observed optically, but the angular distribution of the radiation is much flatter than the distribution of (green) light. The observation of the eclipse also showed that no detectable refraction of the radiowaves is caused by any ionized layer in the moon's atmosphere. Earlier calculations had indicated that such refraction was unlikely.

Large parts of the sky have been charted for 400 Mc/s radiation. Each time the antenna was swung through 30° azimuth at a speed of about 10° per minute. After each such scan the elevation was increased 1°. *Fig. 16* shows a recording obtained with a single scan of the antenna (in this case under slightly different conditions of movement). The chart constructed from all these observations, which extended over several months, is reproduced as *fig. 17* on pages 332-333, together with a detailed

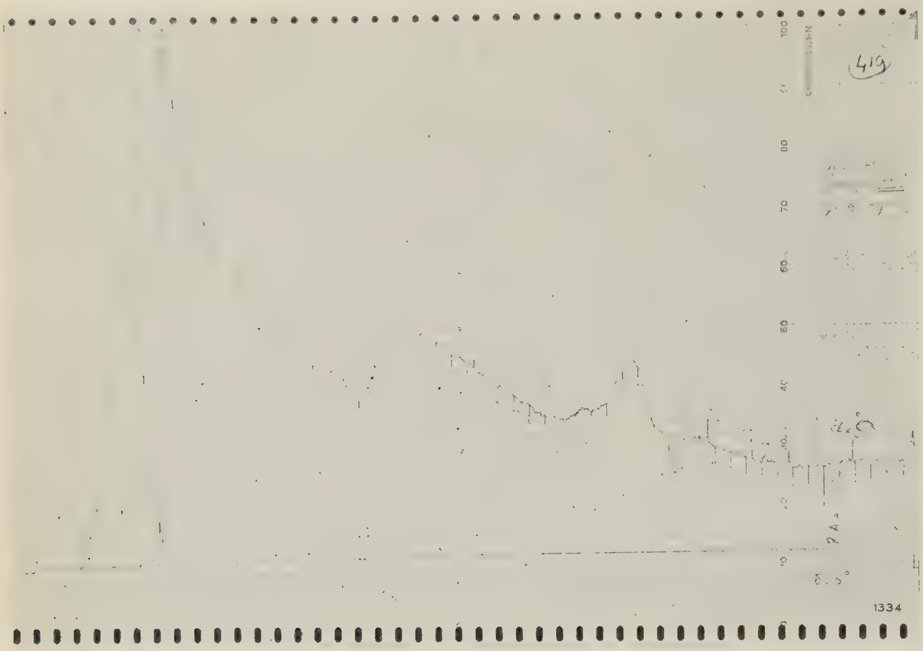

Fig. 16. Recording obtained with the receiver described for a single scan with the 25 m radio telescope at Dwingeloo. The path of the antenna beam for this recording is shown as a dotted line on the overlay sheet for fig. 17. In this case the angle of declination was kept constant at $\delta = 5°$, and the antenna moved at a speed of 8° in right ascension. The degrees marked below the recorded curve refer to right ascension, and those above refer to elevation. In order to be able to record the intensity peak that occurs as the antenna sweeps through the Milky Way, the scale is temporarily displaced by 100 scale divisions.

description. Owing to the very high sensitivity of the installation (low noise factor and high radiation sensitivity) and to the high resolving power of the 25 m reflector, the results now achieved are very much better than was possible ten years ago. The new chart, which incidentally by no means contains all the detailed information extracted from the observations (see below), may be compared with the results of Reber [16]) in 1948; see *fig. 18.*

The chart, fig. 17, is drawn in the form of contours of constant received power (isophots). This power, as already mentioned, is a weighted mean over the antenna beam; it further represents a mean over the frequency band of the receiver, although within the bandwidth of 10 Mc/s the variations of most of the sources observed at 400 Mc/s are negligible. The directional diagram of the antenna contains side lobes in addition to the central beam (see [1]) and [14])). It is possible to compensate for their influence but this correction has not been made in the chart reproduced. As in optical observations, twinkling due to atmospheric influences is also found in radio observations, particularly from the northern direction, where aurora effects occur. This direction was therefore avoided as far as possible; little trouble is experienced from twinkling when the antenna is directed towards the south.

The numbers on the isophots are proportional to the received power; the unit is a flux density of 9.1×10^{-26} W/m^2 per c/s, or an antenna temperature of 1.3 °K. To make the chart easier to read, the isophots are drawn with fairly large intervals. In this way the chart gives a clear picture of the broad structure of the 400 Mc/s radiation received from space, but many small details derived from the observations are lacking in this reproduction and only the strongest "point sources" are distinctly recognizable. The legend to the chart explains various particulars to be read from the contours. The "tails" of the general radiation from our galactic

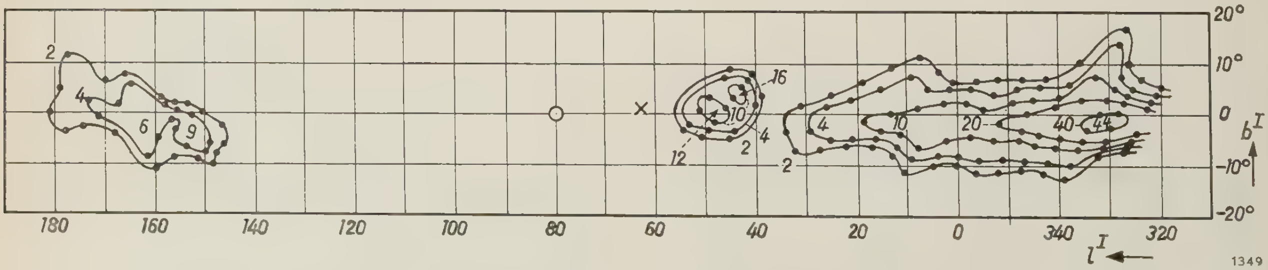

Fig. 18. Chart of the sky for 480 Mc/s radiation, constructed from observations by Reber [16]) in 1948. The chart shows the part of the sky between the same galactic longitudes l^I as in the new chart in fig. 17. The progress illustrated by the latter figure, as a result of the much greater resolution and higher sensitivity of the equipment at Dwingeloo, is evident.

---

[16]) G. Reber, Cosmic static, Proc. Inst. Radio Engrs. **36**, 1215-1218, 1948.

system and the associated apparent anti-symmetry of the Milky Way in relation to its "plane of symmetry", demonstrated by this chart for the first time, deserve particular attention.

A constantly recurring problem in radio-astronomical observations is the occurrence of radio interference, due to transmitters and their harmonics (e.g. in our case radio-sondes between Wales and Copenhagen, and aircraft transmitters between the West of England and South Germany) and to secondary causes, such as the ignition systems of vehicles at distances up to 5 or 10 km away. Even in Dwingeloo, which is fairly remote from busy areas, 25% of the observation time at night has been lost through interference. (During the day observations of weak sources in and beyond the galactic system are not possible because of the intense radiation from the sun.) The same difficulties are experienced elsewhere, and the subject has fortunately attracted international attention. On a proposal of the Netherlands the C.C.I.R. (Comité Consultatif International des Radiocommunications), the technical advisory body to the Post Offices of various countries, has accepted a recommendation to reserve certain frequencies for the purposes of radio astronomy. At the last meeting, concluded 21st December 1959, of the I.T.U. (International Telecommunication Union) which is the body responsible for frequency allocations, certain frequency bands were in fact allocated exclusively for radio astronomy, and other frequency bands were indicated for radio astronomy together with non-interfering services, e.g. beam-approach installations on airfields. Time will show whether this allocation will meet with the necessary international cooperation. In view of the common interest in the science of radio astronomy, which has flourished so enormously in the last ten years, this cooperation may well be expected.

Summary. The article describes a simple, stable and sensitive receiver for the frequency range from 200 to 500 Mc/s (150 to 60 cm), possessing a very low noise factor ($F = 2.5$ at 400 Mc/s), which makes possible accurate observations of the very weak radio waves received from extra-terrestrial sources. The receiver operates on the superheterodyne principle, with an intermediate frequency of 50 Mc/s. The high-frequency amplifier contains two EC 57 disc-seal triodes in cascode, the effective cathode resistance of the second valve being made very high by a simple neutralization circuit. This arrangement provides a very high gain and virtually eliminates the noise contribution from the second valve. Various measures, including the use of a constant-impedance detector and frequency stabilization of the local oscillator with a quartz crystal specially designed for observations at 400 Mc/s, make the receiver so stable that its sensitivity shows no noticeable drift for weeks on end. For calibrating the detector the I.F. amplifier contains a calibrated attenuator, adjustable in steps of 1 dB. The receiver can be given a bandwidth of 10 Mc/s or 1 Mc/s, and the time constant can be varied between 0.1 and 10 sec.

Various radio-astronomical observations are described that have been made with this receiver, particularly in conjunction with the 25 m parabolic reflector of the Radio Observatory at Dwingeloo. When this came into operation in 1956, it was the largest rotatable radio telescope in the world. The isophot chart of the sky drawn from the observations made with this radio telescope, and reproduced in this article, provides the most detailed information at present available on the structure of our Galaxy, measured at 400 Mc/s. Particularly remarkable phenomena are various tails of the general radiation from our Galaxy, and associated with these the antisymmetry of the Galaxy in relation to its "plane of symmetry." The absolute level of the measured radiation intensities is determined by calibration with the aid of a horn antenna: the radio star Cassiopeia A, the most powerful object in the radio sky at these wavelengths, gives a flux density of 56×10^{-24} W/m^2 per c/s.

Fig. 17. The distribution of the radio brightness of part of the sky, observed at 400 Mc/s with the 25 m radio telescope at Dwingeloo. The contours represent isophots (lines of constant received power). The numbers on the contours indicate the power, the unit *) being 9.1×10^{-26} W/m^2 per c/s, or 1.3 °K.

The region of the sky reproduced here comprises part of the Northern Milky Way. For guidance the transparent overlay sheet is marked with some of the most familiar objects in this region of the sky; the Milky Way itself is shown in grey shading, and its plane of symmetry runs through the approximately horizontal dot-dash line. The degrees along the horizontal axis indicate the galactic longitude (l^{I}), and on the vertical axis the galactic latitude (b^{I}). In the direction of the circle C lies the centre of the Milky Way, as seen from our point of observation, and in the direction of A lies the anti-centre. The stars in our vicinity travel, in their general rotation, around the centre of the Milky Way in the direction of B ($l^{\mathrm{I}} = 57°$). A large part of the Milky Way as seen from Dwingeloo never comes above the horizon. This limitation of the area of the sky accessible to observation is indicated by the line on the right. The "practical" horizon shown is somewhat higher than the theoretical horizon, owing to the fact that the observations very close to the horizon are rather inaccurate. The dashed line $\delta = 5°$ (Meas. No. 419) denotes the path described by the antenna for obtaining the recording shown in fig. 16.

Some particulars to be deduced from the radio chart are outlined below.

1) The 400 Mc/s radiation is strongly concentrated around the (symmetry) plane of the Milky Way. Further, the radiation in this plane increases very considerably towards the direction of the centre.

2) The strongest point sources, or regions with high local intensity, are situated near the plane of the Milky Way. It is known that most sources seen on the chart are large regions of hot ionized gas surrounding the bright stars. These are the so-called H II regions (ionized hydrogen), familiar in classical astronomy. Apart from the exceptions discussed below, all identified radio sources (the names are printed in red) are of this type. It has not been possible to determine the true size of any of these sources; they cover a much smaller angle than the antenna beam used in the mapping of the chart. Most of the point sources clearly distinguishable as such are relatively near the sun (at distances of less than 4000 light years). For the most part they are comparatively weak radiators, but their proximity makes them seem relatively powerful. Some of these H II sources have been found to be multiple or composite sources, either by radio investigations at even greater resolving power (G. Westerhout, B.A.N. No. 488 of 31st Dec. 1958) or by optical observations. Cygnus X, for example, consists of a dozen or more separate, although closely adjacent, H II regions.

3) Four of the radio sources, whose identity is given below, differ entirely in their nature from the kind just discussed. Unlike H II sources, these four are brighter at long waves than at short.

Cassiopeia A. Except at short waves, where the sun predominates, this source is the most powerful heavenly object in the whole radio spectrum. Following F. G. Smith's careful localization by means of radio observation, Baade and Minkowski have examined the source with the 200″ Palomar telescope. They found it to be a wispy, roughly spherical shell, consisting of somewhat cirrus-like gaseous clouds, and rapidly expanding at radial velocities of several thousand kilometres per second. The source lies about 10^4 light years away in one of the outer spiral arms of the Milky Way. It is believed to be the remnants of an exploded star, or nova. Incidentally, the isophot 300 of this source gives a very accurate picture of the transverse section at half the peak intensity of the antenna beam, since it is known that this radio source has a diameter of only $^1/_{12}$th degree and that it is very much more powerful than any other source in the immediate vicinity.

Cygnus A. Although this radio object in the sky appears to be the second in brightness, in reality it is the most powerful radio source known. This object, too, has been identified with certainty as a result of the work of Smith, Baade and Minkowski: it consists of two galactic systems in collision at a distance of 10^9 light years. If they were somewhat further away, they would not be observed with the present-day optical telescopes, but they would still easily be "seen" by the radio telescope.

Taurus A. The celebrated Crab Nebula, several times referred to in this article (fig. 2) consists of the remains of a vast stellar explosion (supernova), about 4000 light years away. As mentioned, this Nebula emits synchrotron radiation.

IC 443. This is another cirrus-like gaseous object. Its identification with the radio source seems well established, but the origin of the radiation is not yet clear.

4) Within about 60 degrees of longitude from the centre of the Milky Way the level of the total radio-wave radiation increases towards the centre to a fairly flat maximum, as mentioned under (1). It is known from observations at high and low frequencies that at least two different mechanisms contribute to this radiation. An appreciable part of the 400 Mc/s radiation observed here can be attributed to H II regions which, in the direction of view, are distributed over our entire galactic system, but the major part belongs to a background which must have an entirely different origin. The spectrum of this second kind of radiation shows an intensity that increases with increasing wavelength, rather like the radiation from the sources mentioned under (3). The cause of this non-thermal radiation has not yet been explained, although there are various reasons for assuming that it bears a relation to a general magnetic field in the Milky Way and to particles of very high velocity such as occur in cosmic radiation. This is the radiation component discovered in about 1930 by Jansky, the pioneer of radio astronomy, and which in later investigations was found to be characteristic all of galactic systems of the same type as our own. In the middle of the region from which this non-thermal radiation comes, there is another powerful H II source, Sagittarius A. This source is very close to the centre of rotation of the Milky Way.

5) Of the large galactic systems outside our own, the nearest is M 31, the Andromeda Nebula. Its position is marked on the overlay sheet. Although this object can be clearly distinguished in our recordings, it is barely visible in the chart owing to the comparatively large intervals between the isophots drawn, the more so since the same region of the sky contains a small arm of radiating material which appears to belong to our own Galaxy.

6) A remarkable feature, shown on all radio charts made at these wavelengths since the early work of Reber, is the protuberance indicated by the dashed vertical line D. Our chart shows more structural details of this than any of the earlier charts, owing to the higher resolving power and sensitivity of our equipment, and perhaps also as a result of the brightness distribution being different at other wavelengths.

This radio protuberance has no counterpart in the optical picture of the Milky Way, and its origin is quite unknown. It is not even certain whether it consists of a local bulge or whether it is a peculiarity in the shape of the entire Milky Way. There is another phenomenon to be seen, and this was first noticed when making the present chart: this protuberance seems to be echoed in a systematic manner by two similar but weaker protuberances in the directions indicated by the dashed lines F and H.

On the whole it can be said that our galactic system possesses a high degree of symmetry, both optically and in terms of radio waves: it has rotational symmetry and moreover possesses a mirror plane of symmetry. The protuberances referred to are a notable exception to this rule: radio waves, of relatively low intensity, are found only on one side of the plane of symmetry, up to a large galactic latitude. Further, the northern protuberances D and F appear to be accompanied by two minima, E and G, which occur at the same galactic longitude, at southern galactic latitudes. This markedly antisymmetrical distribution of the radiation is a characteristic of the radio Milky Way which, until the completion of this chart, had gone more or less unnoticed. Comparable charts made at much longer wavelengths show the effect to nothing like the same extent. Whether it also occurs at much shorter wavelengths is not known, radio telescopes not yet being sensitive enough for such observations.

---

*) This value (the proportionality coefficient in the relation, found by calibration, between the output voltage and input power of the receiver system(has an estimated error of ± 15%. In this connection see the thirdarticle mentioned in 15)). The estimated error in the scale zero-point is 10 to 15 °K.

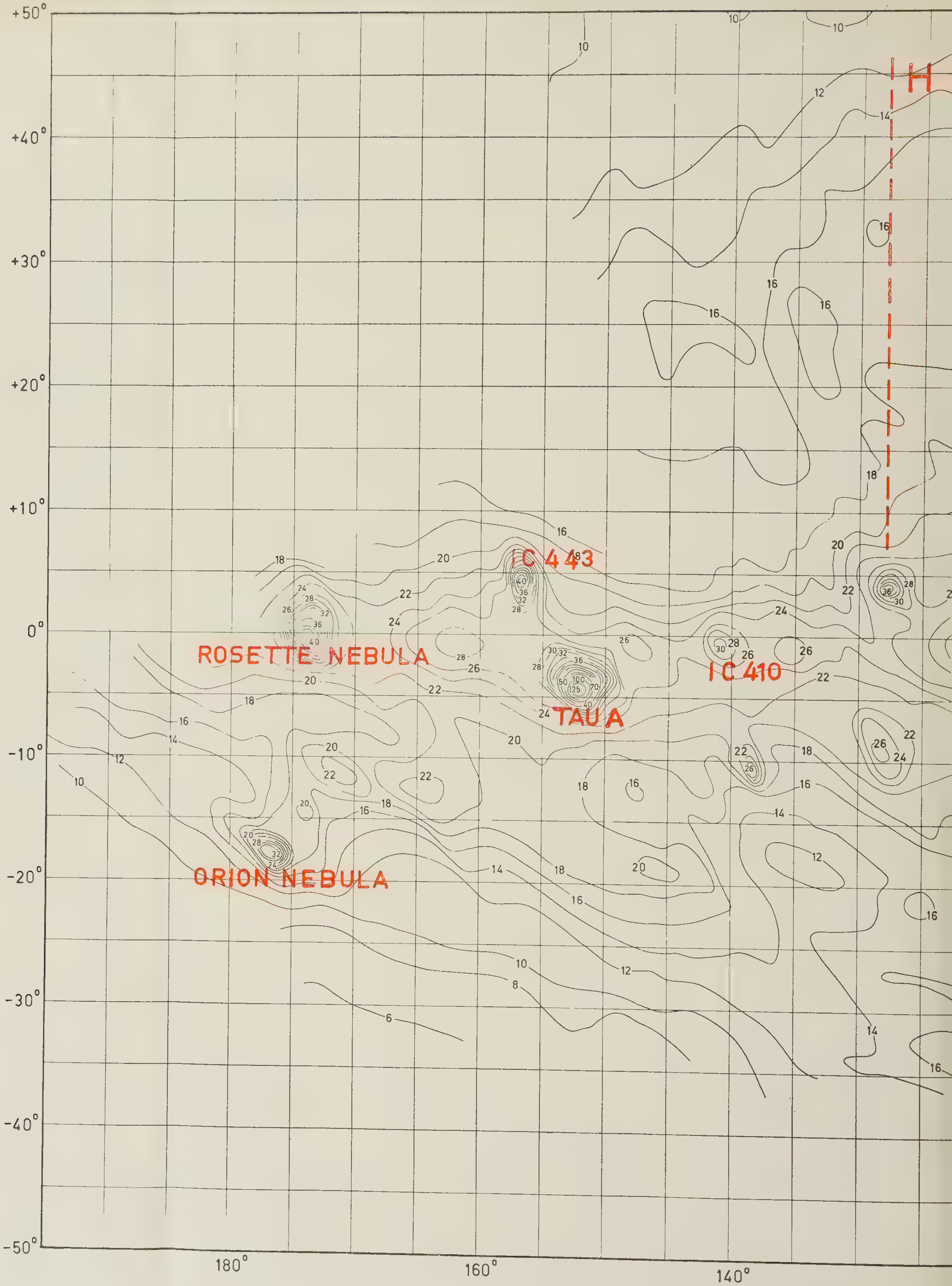
+50°
+40°
+30°
+20°
+10°
0°
-10°
-20°
-30°
-40°
-50°
180°
160°
140°
IC 443
ROSETTE NEBULA
TAU A
IC 410
ORION NEBULA
H

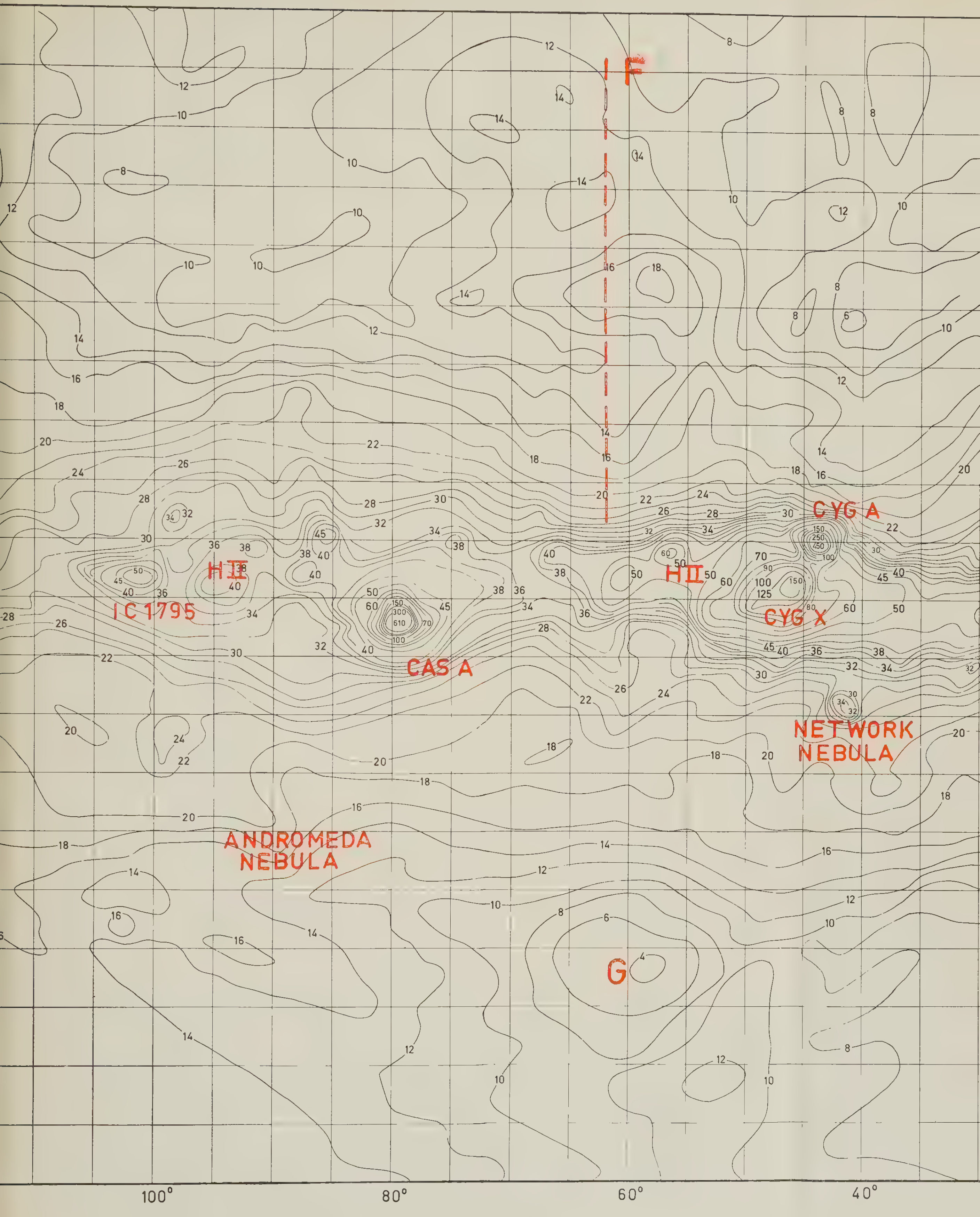
F
G
IC 1795
H II
CAS A
H II
CYG A
CYG X
NETWORK NEBULA
ANDROMEDA NEBULA
100°
80°
60°
40°

THE FRUITS AND FOUNDATIONS OF SOLID-STATE RESEARCH

by D. POLDER.

539.2:54-16

The article below broadly reproduces the text of the address delivered by the author on 2nd Dec. 1959 upon his inauguration as extra-mural professor at Delft. With a few examples the author illustrates the significance of the solid state in electrotechnical applications. He then surveys the evolution of the theory that forms the basis of any discussion of solid-state phenomena. With Professor Polder's kind cooperation, the text is supplemented here by a concise bibliography.

"Germanium, atomic number 32, atomic weight 72.6, melting point 958 °C, specific gravity 5.35, had already been predicted by Mendeléeff as eka-silicon before it was discovered by Winkler in 1886." So reads the first sentence of the article on germanium in the sixth edition of the Dutch Winkler-Prins Encyclopaedia, published in 1950. The last sentence of the article is also worth quoting; it reads: "The element has no practical value whatsoever." Taking into account that the publication of this edition was delayed by the Second World War, it is fair to assume that this sentence broadly represents the state of affairs some fifteen years ago. Now, in 1959, more than a hundred-million transistors a year are produced from the element germanium in factories all over the world. Germanium, which for years had received only passing mention in text books of chemistry, and whose physical properties had been studied only superficially, may now justly claim to be the most thoroughly investigated, chemically, physically and technologically, of all the solids.

Germanium is a semiconductor. Before 1940 the effects occuring in semiconductors were still in many respects perplexing. The electrical conductivity of these substances was much smaller than that of metals, and yet too large to allow them to be classed as insulators. In some cases the conductivity was found to be virtually independent of temperature, and in others it increased very markedly with temperature, an effect unknown in metals [1]). Deviations from Ohm's Law were often found even at very low current densities. The worst was that the behaviour of these already somewhat strange chemical substances proved to be so sensitive to impurities. Many a right-minded physicist was therefore inclined to regard the phenomena in semiconductors with deep suspicion.

The unusual conduction properties of semiconductors had meanwhile attracted the attention of those who were engaged in the search for curious properties of matter that might be capable of practical application. The negative temperature coefficient of the resistance of oxidic semiconductors was turned to good use for limiting the heater current when switching-on a thermionic valve [2]). The non-linear electrical characteristic of certain semiconductors found application in the crystal diode, which became an invaluable aid in the detection of radar signals [3]). It was in this connection, during the war, that germanium was first studied systematically as a semiconductor. And it was the demand for practical applications that attracted to fundamental semiconductor physics the attention which many physicists had not believed it deserved.

The great moment in the history of semiconductors came in 1948 when, as the result of their work in the Bell Laboratories, Shockley, Bardeen and Brattain announced their discovery of transistor operation [4]). This discovery led to the possibility of making a piece of germanium fulfil the function of a thermionic valve. As an amplifier of electric signals the germanium transistor now rivals the valve. In itself, transistor operation is a most remarkable physical phenomenon. Moreover, it is a very well understood phenomenon, which is in no way bound to the specific chemical properties of the element germanium. In principle it can also occur in other elementary semiconductors and in semiconducting compounds.

The advent of the transistor has profoundly influenced the recent development of solid-state physics. The intensive study of all possible kinds of semiconductors in laboratories far and wide [5]) is one direct result. Seen more broadly, the existence of the transistor and associated semiconductor devices has focused attention very sharply on the many and varied technical potentialities of solid-state properties, and in particular of those properties bound up with the behaviour of electrons in solids. It would be wrong to assume, however, that the technical possibilities of solids in electronic engineering had scarcely been recognized before the transistor came on to the scene. The extensive work done and still being done, in the Netherlands [6]) and elsewhere, on oxidic semiconductors and magnetic materials, testifies to the contrary. The applications of magnetic materials extend over the whole frequency range of electromagnetic waves covered by electronics. Research on magnetism, including fundamental research, is strongly influenced by the demand for technical applications. On this the transistor has had no bearing at all.

In a wider context than that of solid-state research, the transistor is held up as striking evidence of the truth of the assertion that those in search of phenomena that can be turned to practical use should devote themselves to pure scientific research. The first sentence of the introduction to Shockley's celebrated book on transistor physics [7]) reads: "If there be any lingering doubts as to the wisdom of doing deeply fundamental research in an industrial laboratory, this book should dissipate them." It is not difficult to enumerate aspects of the invention of the transistor that support this assertion. One can say that the transistor effect found in the element germanium was a particularly surprising one, and it was recognized for what it was only because it was discovered in the course of a systematic fundamental investigation. One can further maintain that the exploitation of the effect to a technically useful application was possible only because of the complete and fundamental understanding of the physical effect. It is more difficult to indicate *how* fundamental the research should be in an industrial laboratory [8]). There is another sentence in the introduction to Shockley's book that should not be overlooked in this connection; it reads: "But there should be no illusions about the necessity of a large measure of good luck".

Whatever one might think about the relation of science to industry, there is no denying that solid-state research has increased enormously since the discovery of the transistor, and that much pure scientific work is now being done in the large industrial laboratories. The interest in the solid state, shown by large and small industrial undertakings and by some governmental departments, appears for example from the many advertisements in American journals and magazines that hold out solid-state research to the physicist as a chance of beginning a rewarding career in industry. The advertisements are interesting, too, in that they give a fairly reliable indication of the subjects at present being studied: infra-red detectors, solid-state microwave amplifiers, thermoelectric cooling, data storage elements, high-frequency diodes, the theory of "devices", photoconductors, semiconductor technology, thin magnetic films. These are only a few of the subjects that are engaging the special attention of the electronics industry.

In describing the fortunes of a single chemical element, germanium, I have tried to give some idea of the vigorous developments that are taking place in the whole of the solid-state field. The example chosen has allowed me to emphasise the great stimulus which research has received from the demand for technical applications. Fortunately, there are many fields of solid-state physics that have grown without this stimulus. I say fortunately, not because I deplore the stimulus or regard it as secondary, but because I feel it is a good thing for scientific curiosity that it does not have to depend on such a stimulus. To give an instance I shall discuss briefly a subject which is studied mainly at the Universities.

After the last world war, research was started at the Clarendon Laboratory, Oxford University, on the absorption of microwaves in paramagnetic salts [9]), use being made of the facilities created by the wartime development of radar engineering. From the theoretical work of Van Vleck, from susceptibility measurements and measurements of specific heat at low temperatures, it had long been known that the energy levels of paramagnetic ions in crystals may lie very close together [10]). In order to determine these levels by direct spectroscopic means, electromagnetic waves of wavelength about 1 cm are needed. Microwave absorption, or paramagnetic resonance, was therefore at that time primarily microwave spectroscopy. The microwave investigations undertaken at Oxford and many other places have now taken on a much wider significance. A subject of investigation of great interest at the present time is the mechanism of relaxation; this is concerned with the rate and the nature of the processes that tend to restore thermal equilibrium between the various energy levels. Another subject at present receiving widespread attention is the use of the paramagnetic resonance technique, and of the associated method of nuclear magnetic resonance, for studying the structure of matter [11]). In research on the structure of impurities and other lattice imperfections, these resonance techniques have proved to be particularly valuable. Here we have an example of an academic application of academic research.

It is interesting to note that resonance investigations have also led to a number of technical applications. Nuclear magnetic resonance, for instance, is used in the chemical analysis of mixtures of organic compounds, e.g. in the oil-refining industry. Another application, which I shall deal with at greater length, is based on a discovery made by Bloembergen of Harvard University. From Townes' work on the microwave absorption of gas molecules it was known that, under certain conditions, molecules in a microwave field will emit instead of absorbing radiation [12]). This is the phenomenon known as stimulated emission. Since the stimulated emission is *coherent* with the incident electromagnetic wave, the effect can be used for amplifying the incident signal. In the *maser*, which is an acronym for *m*icrowave *a*mplification by stimulated *e*mission of *r*adiation, the fundamental phenomenon of stimulated emission was specifically put to use for the first time. A necessary condition for obtaining a *nett* emission is that, of the two molecular energy levels involved, an excess of molecules should on average occupy the upper level. In thermal equilibrium the opposite is the case. The reversed occupation density required must therefore be brought about by some artifice. Bloembergen set out to see whether the maser principle could also be realized in a paramagnetic salt [13]). From the work on microwave spectroscopy a great deal was known about energy levels having energy differences of the appropriate order of magnitude. The study of paramagnetic relaxation at the temperature of liquid helium had shown that it must be possible here, too, to achieve the necessary reversed occupation, and by a relatively simple microwave technique. Once Bloembergen's ideas on the solid-state maser had become known, this new microwave amplifier was in fact successfully demonstrated at various places. The special interest shown in the maser in technical circles, in spite of the objections to working with liquid helium, is explained by the fact that masers are amplifiers possessing, in principle, very low inherent noise. For amplifying extremely weak signals from extra-terrestrial sources this is a feature of the utmost importance.

In the foregoing we have touched on two amplifiers, the transistor and the maser, both of which exploit the properties of the solid-state. This will allow us compare the principles underlying the amplification in these and other devices. The transistor, like the thermionic valve, operates in the first instance with a continuous current which is periodically varied by an alternating current signal in such a way that the signal thereby performs virtually no work. The energy delivered by the amplified signal originates in the source which supplies the continuous current. Of course, the mechanism causing the current to flow through the valve differs from that which maintains the flow of current in a transistor. In the valve the current is produced by an electric field, whereas in the transistor the current is the result of a concentration gradient of charge carriers injected in a semiconducting layer. Nevertheless, the transistor and the thermionic valve, regarded as four-terminal networks, have much in common.

The maser, on the other hand, is a true negative-resistance amplifier. To be more precise, in the maser the paramagnetic salt behaves in relation to the signal like a tuned circuit, consisting of a negative resistance, a negative inductance and a negative capacitance. In itself this combination has the same characteristics as a tuned circuit composed of positive elements, but the moment it is loaded with a positive resistance it can be used as a generator or amplifier of electromagnetic oscillations. Of course there is no question of getting something for nothing. To trace the energy source of a negative-resistance amplifier, we must look into the physical cause of the negative resistance. In the maser we find at once that the energy is supplied by the stimulated transitions of the molecule or paramagnetic ion from a higher to a lower energy level. The ingenious mechanism which sustains the reversed occupation introduces into the system the energy required for amplification.

The great difference between amplifiers of the thermionic valve and negative resistance types is that, in the first type, changes in the output circuit scarcely influence the input signal, whereas in the second type that is just what they do. Since the absence of feedback may be an important practical requirement, it is desirable to complement the negative-resistance amplifier with directional isolators or "unilines". These are network elements which transmit signals coming from one direction but not from the other. Under certain conditions, solids in thermodynamic equilibrium exhibit the non-reciprocal properties needed for constructing a directional isolator [14]). The classic example is the microwave uniline devised by Hogan which exploits the non-reciprocal permeability tensor in pre-magnetized ferrites [15]). In an analogous way one can use the non-symmetrical resistance tensor of a semiconductor located in a magnetic field [16]).

In this connection it may be noted that, in recent years, special attention has been focused on amplification by means of solid-state negative resistances. It is hoped that this will offer new possibilities for amplifying signals of exceptionally high frequencies.

A very recent example is the *tunnel diode* invented by Esaki in Japan [17]). A tunnel diode is a semiconductor built in such a way that somewhere over a layer no more than 100 Å thick the current can flow only because of the quantum-mechanical tunnel effect. Cutting-off the tunnel current by raising the applied voltage gives rise to a negative differential resistance. Another example is the parametric amplifier [18]). Like the maser, a parametric amplifier behaves in relation to the applied signal in the same way as a circuit composed of entirely negative elements. As opposed to the maser or the tunnel diode, the formal negative resistance in a parametric amplifier is not due to the physics of a resistance element. An essential feature of the parametric amplifier is that it should contain a capacitance, an inductance or some other reactive element whose value varies together with the applied voltage or current. The energy required for the amplification is supplied by an alternating-current source whose frequency differs from, and is usually higher than, the frequency of the signal to be amplified. The operation of this type of amplifier can be demonstrated by a simple calculation. It seems, however, that this calculation is not so obvious, in view of the fact that the parametric or reactance amplifier has been repeatedly discovered in the course of this century and again forgotten. In recent years it has been found that solid-state parametric amplifiers can be made which operate at microwave frequencies. The amplifier devised by Suhl, which led to the recent revival of this type of amplifier, uses the ferromagnetic resonance phenomenon [19]). An amplifier using a variable capacitance can be made with a suitable designed semiconducting diode. In this case the variable capacitor is the semiconductor itself, which is provided with a thin, poorly conducting layer whose thickness varies with the applied voltage. The present interest in parametric amplifiers springs from the fact that, like masers, they are characterized by very low inherent noise [20]).

The practical value of the properties of the solid state extends over a very wide field. In discussing a few modern applications in electronic engineering I have, of course, done less than justice to the versatility of the existing practical applications. I have chosen my examples from a restricted field, and they were all concerned, directly or indirectly, with the amplification of electromagnetic signals. The new developments in metallurgy, to mention just one instance, have not even been referred to in passing. Versatility is the characteristic of the applications and of the properties of the solid state; and versatility also distinguishes the theory of the solid state.

I should now like to touch briefly on the theory. It is not my intention to go into details of the numerous and often specialized concepts with which the solid-state theoretician is concerned. Not that I believe that solid-state theory can be discussed only in terms of elegant — or cumbersome — mathematical formulae. On the contrary, I am convinced that any bit of theory that is really well understood lends itself to an interpretation in which formulae play only a very minor part. I believe, too, that a theoretician working together with his experimental colleagues on solid-state research should always try to arrive at this sort of non-formal interpretation of the theory. I cannot discuss details of theoretical concepts here because such a discussion takes time, the time needed to bring out the nuances of a concept and to deal with the underlying assumptions and restrictions.

I should therefore prefer to say something about the *structure* and *elements* of solid-state theory [21]). Strictly speaking it is quite wrong to speak of *the* theory of solids. It might rather be asserted that there is in fact no one theory of the solid state. After all, there is good reason to believe that the fundamental laws of physics, in particular the theory of the electron and of the electromagnetic field, wave mechanics and the discipline of statistical mechanics and its associated subject, thermodynamics, are in principle capable of explaining virtually all the phenomena of the solid state. The fact that this does not turn out to be so easy in practice is due not to any limitation in the validity of the fundamental laws, but to the inadequacy of existing techniques for applying these laws to so complicated a system as a solid. Let us regard for a moment the physical phenomena of the solid state as a melting pot for the theory of solids. We throw in all the basic subjects of theoretical physics. What finally emerges is not a beautifully formed single crystal of solid-state theory but a somewhat amorphous mass studded here and there with a number of serviceable crystallites. These crystallites are the theories of the solid state. The fragments of theory show a certain interrelationship, but they by no means fit together neatly at every point. Each fragment is a model, encumbered by numerous simplifying assumptions and abstractions.

According to the nature of the models the theories of the solid state can be variously classified. One can distinguish, for instance, between macroscopic-phenomenological theories and atomistic theories.

In a macroscopic theory, the existence of electrons and atoms is ignored. A typical example is the theory of elasticity. Atomistic theories may be subclassified into lattice theories and electron theories. From a theoretical viewpoint this classification relates to the mass of the studied particles. A lattice theory is concerned with the interrelationship and motion of the *heavy* particles, the atoms, and avoids as far as possible a detailed discussion of the behaviour of electrons. A typical lattice theory is that of Born and Madelung on the cohesion of ionic crystals. It dates from 1912, the time when Von Laue and Bragg were working on the diffraction of X-rays in solids. The theory of lattice vibrations and of the specific heats of crystals was greatly advanced by the discovery, at the beginning of this century, of the elementary quantum of action *h*. The models of Einstein and Debye relate the quantum characteristics of the harmonic oscillator to the existence of a finite number of modes of oscillation in a solid.

The theory of the *imperfect* lattice was a relatively late development. The concept of dislocations, originally introduced to explain plastic deformation, has proved to be particularly fruitful, and its help is invoked for explaining many other phenomena in imperfect lattices. The dislocation, a partly atomistic and partly macroscopic concept postulated by Taylor in 1934, has become a most essential element of the theory of solids [22]).

The advent of wave mechanics in about 1925, and the associated theory of electron spin and Fermi-Dirac statistics, had a revolutionary effect on the theories concerning the behaviour of the *light* particles in solids, that is on the electron theories of the solid state. The modern theory of electrons in solids stands or falls with the quantum-mechanical method of description. On the one hand there is the quantum theory of ferromagnetism and paramagnetism, in which the properties of the electron spin are the focal point. On the other hand there are the wave-mechanical theories on bound and free electrons. The most representative of these is the energy band theory, evolved by Bloch and others about 1930, which is based on the wave-mechanical model of mutually-independent electrons in a periodic potential field. The band theory explains, in principle, the existence of metals, semiconductors and insulators. It leads to the concepts, so important for semiconductors, of hole and electron conduction. It also affirms that electrons in a periodic potential field have an infinitely long free path. Without this latter idea modern *transport theory* could not exist. In the theories on the transport of charge carriers in solids an essential role is played by the interaction between electrons and atom movements. This interaction is again of particular interest at the present time: the phenomenon of superconductivity, which is gradually becoming better understood, is very subtly related to it [23]).

I have tried to show that the important and new ideas that have come into theoretical physics with quantum mechanics have helped fundamentally to form the present-day theoretical picture of the solid state. It is worth noting that this picture has undergone very little change during the recent period of boom in solid-state research. The theory of solids is rather going through a period in which ideas are being refined and elaborated, and in part cast in a more quantitative mould. In this way semiconductor research has led to further detailed elaboration of the band theory and transport theory. For example, the problem of the effect of a uniaxial compression on the fine structure of the Zeeman effect of indirect excitons in semiconductors, involves the theory in a most detailed form.

It is not to be inferred from this, however, that the theory of solids has now assumed a more or less definitive shape. In the first place, we know from experience that important consequences of an existing theoretical picture may go unnoticed for many years. Transistor action is a case in point. At the time of its discovery, the theory of transistor action fitted very well into existing ideas on the solid state, but it was evolved only after experiments had drawn attention to the existence and significance of the finite recombination rate of holes and electrons in a semiconductor, on which the transistor action depends.

Further, quantitative questions still await answers. What is the magnitude of the work-function of caesium-antimonide? How large is the activation energy of a vacancy in copper? What is the band structure of bismuth-telluride? Such quantitative questions still present the theoretician with a challenge. In attempting to answer them, he cannot get very far with general considerations. Calculations on this kind of problem so often involve doubt as to the effect of the simplifying assumptions inevitably used that little confidence can be placed in the final result. It may be that electronic computers will help in this respect by establishing empirically the relative merits of the many possible methods of calculation, by comparing the results with known experimental data. Obviously, however, the computer cannot answer the question of *why* one method appears to produce better results than another.

There are also a number of very fundamental questions that have not yet been satisfactorily resolved. For instance, there are good experimental reasons for assuming that the mechanism of conduction in various oxidic semiconductors cannot be described in terms of the transport theory derived from the band theory 24). Now it is true that this theory, so successful in its application to germanium and silicon, does in fact have its limitations. It assumes the existence of mutually independent electrons which are only *weakly* bound to the lattice. One may therefore ask what form the theory should take in the case of conduction with electrons which interact *strongly* with each other and with the lattice. There is an evident need here for a simple and realistic model that will throw light on this problem,

It is for the theoretician to devise such a model, a model which, as always, should be simple enough to allow of mathematical treatment, and at the same time realistic enough to demonstrate the essential nature of the phenomenon to be described. It is interesting work, in which the theoretician is time and again compelled to take into account the nuances, the assumptions and the limitations of the concepts he wishes to use. It is interesting, too, in that he may perhaps be able, very indirectly, to contribute in some measure to the creation of new applications of solid state physics.

BIBLIOGRAPHY

1) G. L. Pearson and W. H. Brattain, History of semiconductor research, Proc. Inst. Radio Engrs. **43**, 1794-1806, 1955.

2) E. J. W. Verwey, P. W. Haayman and F. C. Romeyn, Semiconductors with large negative temperature coefficient of resistance, Philips tech. Rev. **9**, 239-248, 1947/48.

3) H. C. Torrey and C. A. Whitmer, Crystal rectifiers, Radiation Laboratory Series, No. 15, McGraw-Hill, New York 1948.

4) J. Bardeen and W. H. Brattain, The transistor, a semiconductor triode, Phys. Rev. **74**, 230-231, 1948, and the book by Shockley under footnote 7).

5) See the series of articles in the transistor issue of Proc. Inst. Radio Engrs. **46**, 949-1300, 1958 (No. 6).

6) For oxidic semiconductors, see for example E. J. W. Verwey and F. A. Kröger, Philips tech. Rev. **13**, 90-95, 1951/52. For magnetic materials see: J. J. Went and E. W. Gorter, Philips tech. Rev. **13**, 181, 1951/52; J. J. Went, G. W. Rathenau, E. W. Gorter and G. W. van Oosterhout, Philips tech. Rev. **13**, 194, 1951/52; G. H. Jonker, H. P. J. Wijn and P. B. Braun, Philips tech. Rev. **18**, 145, 1956/57; J. Smit and H. P. J. Wijn, Ferrites, Philips Technical Library, 1959.

7) W. Shockley, Electrons and holes in semiconductors, with applications to transistor electronics, Van Nostrand, New York 1950.

8) See H. B. G. Casimir, Science and Industry, Philips tech. Rev. **20**, 85-88, 1958/59.

9) B. Bleaney and K. W. H. Stevens, Paramagnetic resonance, Rep. Progr. Phys. **16**, 108-159, 1953. K. D. Bowers and J. Owen, Paramagnetic resonance II, Rep. Progr. Phys. **18**, 304-373, 1955.

10) H. B. G. Casimir, Magnetism and very low temperatures, Cambridge Univ. Press, London 1940.

11) See, for example, J. S. van Wieringen, Paramagnetic resonance, Philips tech. Rev. **19**, 301-313, 1957/58; D. J. Kroon, Nuclear magnetic resonance, Philips tech. Rev. **21**, 286-299, 1959/60 (No. 10).

12) J. P. Gordon, H. J. Zeiger and C. H. Townes, The maser — new type of microwave amplifier, frequency standard and spectrometer, Phys. Rev. **99**, 1264-1274, 1955.

13) N. Bloembergen, Proposal for a new type solid-state maser, Phys. Rev. **104**, 324-327, 1956.

14) On the principle of non-reciprocity, see B. D. H. Tellegen, The gyrator, an electric network element, Philips tech. Rev. **18**, 120-124, 1956/57.

15) C. L. Hogan, The ferromagnetic Faraday effect at microwave frequencies and its applications — The microwave gyrator, Bell Syst. tech. J. **31**, 1-31, 1952.

16) See for example F. Kuhrt, Eigenschaften der Hallgeneratoren, Siemens Z. **28**, 370-376, 1954; W. Hartel, Anwendung der Hallgeneratoren, Siemens Z. **28**, 376-384, 1954; W. J. Grubbs, Hall effect devices, Bell Syst. tech. J. **38**, 853-876, 1959 (No. 3).

17) L. Esaki, New phenomenon in narrow germanium p-n junctions, Phys. Rev. **109**, 603-604, 1958.

18) See B. Bollée and G. de Vries, Experiments in the field of parametric amplification, Philips tech. Rev. **21**, 47-51, 1959/60 (No. 2).

19) H. Suhl, Proposal for a ferromagnetic amplifier in the microwave range, Phys. Rev. **106**, 384-385, 1957; H. Suhl, Theory of the ferromagnetic microwave amplifier, J. appl. Phys. **28**, 1225-1236, 1957.

20) A. van der Ziel, On the mixing properties of non-linear condensers, J. appl. Phys. **19**, 999-1006, 1948, in particular page 1006.

21) See, *inter alia*, the following textbooks: C. Kittel, Introduction to solid state physics, second edition, Wiley, New York 1957; A. J. Dekker, Solid state physics, Prentice Hall, Englewood Cliffs 1957; F. Seitz, The modern theory of solids, McGraw-Hill, New York 1940.

22) A. H. Cottrell, Dislocations and plastic flow in crystals, Oxford Univ. Press, London 1953.

23) For a synopsis of this extremely difficult subject, see: C. G. Kuper, The theory of superconductivity, Advances in Physics **8**, 1-44, 1959 (No. 29).

24) See G. H. Jonker, Analysis of the semiconducting properties of cobalt ferrite, Phys. Chem. Solids **9**, 165-175, 1959 (No. 2), and S. van Houten, Semiconduction in NiO, to appear shortly in Phys. Chem. Solids.

Summary. Principal contents of the address delivered by the author upon his inauguration as extra-mural professor at Delft. The author takes the work done on germanium to illustrate the enormous development of solid-state research. He points to the impetus received both from industrial applications (transistors, magnetic materials, oxidic semiconductors) and from scientific curiosity (maser, tunnel diode, parametric amplifier), and draws a comparison between the various amplifiers mentioned. Turning to the theory, or rather the theories of the solid state, the author considers various theories concerned with the interrelation and movement of *heavy* particles (lattice theory) and those concerned with *light* particles (electron theories, including the band theory and transport theory). Although there is as yet no comprehensive theory of the solid state, existing theories are being refined and elaborated in many fields. Reference is finally made to the fact that many important problems, both quantitative and fundamental, still await solution.

A METHOD OF GROWING DISLOCATION-FREE GERMANIUM CRYSTALS

by B. OKKERSE.

548.571:546.289

The importance of research into the properties and technology of the semiconductors germanium and silicon is evident when one considers their application in the manufacture of diodes and transistors. The article below describes the method by which single crystals of germanium entirely free of dislocations have been made in Philips Eindhoven laboratories. This article links up with a previous article in this journal, which dealt with the purification and doping of germanium and silicon.

An important aspect of solid-state research at the present time is the study of the way in which the macroscopic physical and physico-chemical properties of crystals depend on the physical imperfections or defects of the crystal lattice. Principal among these defects are: 1) the absence of atoms at sites in the crystal lattice that should be occupied (*vacancies*), 2) the presence of atoms at places that are not lattice sites (*interstitial atoms*) and 3) linear lattice defects or *dislocations*.

The presence of dislocations in the lattice of a single crystal may affect, for example, the mechanical properties, the diffusion of foreign atoms, the rate of alloying and dissolution and also, in the case of semiconductors such as silicon and germanium, the life time of injected charge carriers. Further, depending on the circumstances, the dislocation may act as a sink or as a source of both vacancies and interstitial atoms, and in this way too it may detract from the perfection of the crystal. As far as the semiconductors referred to above are concerned — other materials will be left out of account in this article — research on the relation between crystal imperfections and physical properties is important not only to fundamental science but also to technology, in connection with the manufacture of diodes and transistors.

For the purpose of such research it would be a great help to have a material in which one particular type of lattice defect is entirely absent. This requirement, however, can be fulfilled only in respect of one type of defect: since point defects are thermodynamically stable, only the absence of dislocations enters into consideration.

In this respect germanium is a promising material. In germanium crystals, grown by conventional methods, the dislocation density, i.e. the total length of the dislocation lines in one cubic centimetre, measured in cm/cm^3 or in cm^{-2}, is about 1000 times less than in the most perfect *metal* crystals, the respective orders of magnitude being 10^4 cm^{-2} and 10^7 cm^{-2}. Some time ago it in fact proved possible to make single crystals of germanium entirely free of dislocations. We shall first describe the procedure adopted and the physical principles on which it was based. We shall then discuss the methods by which the crystals made were examined for the absence of dislocations, and we shall present the arguments which lead us to believe that the crystals were indeed free from dislocations. Finally we shall comment briefly on the perfection of the dislocation-free crystals thus obtained.

Method of preparing dislocation-free germanium crystals

The method evolved for preparing dislocation-free single crystals of germanium is simply a special method of crystal-pulling. The pulling apparatus can either be used with an ordinary crucible or with the recently developed floating crucible ¹). After the rotating seed crystal has been brought into contact with the liquid germanium and the pulling process started, the diameter of the growing crystal is gradually reduced to 1 or 2 mm. This is done by gradually raising the temperature of the melt a few degrees. The new situation is thenceforth maintained over a length of growth of about 20 mm. Finally, in a similar way, the diameter is again gradually increased to the required value (*fig. 1*) and the pulling operation is continued until the crystal is the right length. The pulling rate chosen is less than about 1 mm/min, compared with 2 or 3 mm/min in normal crystal-pulling. The flow rate of the inert gas circulating around the crystal must be kept carefully constant. It is also important that there should be no particles of solid matter floating

---

¹) The method of pulling a single crystal from a melt was recently described in this journal in an article by J. Goorissen, Segregation and distribution of impurities in the preparation of germanium and silicon, Philips tech. Rev. **21**, 185-195, 1959/60 (No. 7), in which references to other literature on the subject will be found.

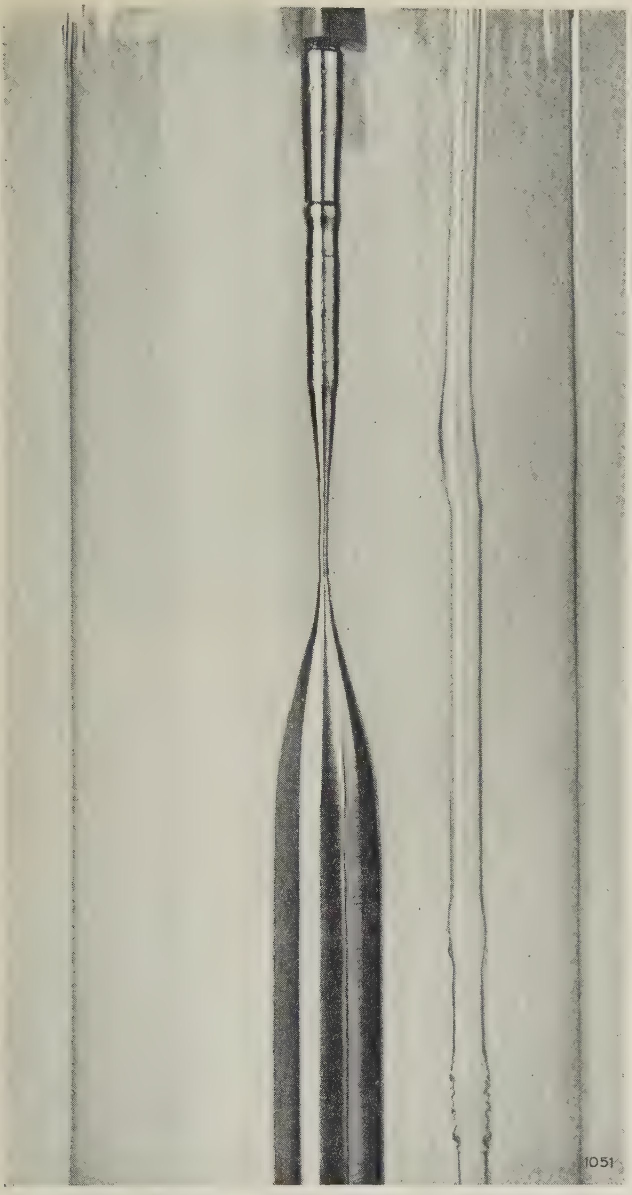

Fig. 1. Dislocation-free single crystals of germanium can be made by the pulling method if the diameter of the first part of the growing crystal is reduced to 1 or 2 mm and this diameter is maintained over a length of about 20 mm. The photograph shows from top to bottom: the seed holder, the seed, the narrowed portion, and finally the dislocation-free portion whose diameter is first gradually increased and subsequently held fixed. (The irregularities in the contours, particularly of the thin portion, are mainly due to the fact that the crystal was photographed through the wall of the glass envelope.)

on the surface of the molten germanium (e.g. germanium oxide or graphite from the crucible).

Physical considerations

The occurrence of dislocations in a crystal presupposes the presence of dislocation sources and mechanical strains. The dislocation sources may be inside the crystal as well as on the surface. A dislocation pinned at two points in the crystal can act as an internal source. A source of this kind can, in principle, give rise to large numbers of ring-shaped dislocations [2]). The nature of the surface sources is not yet clear.

With regard to the mechanical stresses required for the generation of dislocations, it may be noted that in a crystal grown by pulling from the melt these can only be caused by the presence of a temperature gradient. It can be demonstrated [3]) that a temperature gradient produces no stresses only when 1) the heat flux through a crystal is constant, 2) there are no radial heat-losses, and 3) the rate of growth is zero. Obviously, these conditions cannot be fully satisfied in practice. Fortunately, this is not necessary, since the occurrence of growth stresses leads firstly to a merely elastic deformation of the crystal lattice, plastic deformation setting in, i.e. dislocations being created, only when the stress exceeds a certain value [2]).

The reason why the method of pulling described above produces dislocation-free crystals may now be explained as follows. By initially reducing the diameter to 1 or 2 mm, and by pulling the crystal slowly, we approach the conditions that must be satisfied for the thermal stresses to be zero. Evidently, this is done in such a way that the lattice undergoes only elastic deformation and the generation of new dislocations from the existing sources is prevented. The dislocations present in the seed crystal are prevented from growing further down the crystal by making the thin section of the crystal long enough: those dislocations which intersect the solid-liquid interface at a given moment will normally grow further into the subsequently solidifying part of the crystal, but the thin neck of crystal increases the chance that they will intersect the crystal surface and thus "grow out" of the crystal (cf. *fig. 2*).

In the next part of the pulling operation, during which the diameter of the crystal is again enlarged and finally held constant at a relatively large value, the thermal stresses are certainly not small. It is difficult, however, to generate dislocations in a dislocation-free germanium crystal. Even if such a crystal is thermally "mishandled", e.g. by pulling it abruptly out of the melt during growth, dislocations are still not produced in it [4]). If, on the other hand, this experiment is done on a crystal having a dislocation density of about 10^4 cm^{-2}, the density increases to 10^6 or 10^7 cm^{-2}.

A remarkable effect is found if the melt contains floating solid particles and these collide against the growing crystal. The part of the crystal produced after the moment of contact is found to contain a continually expanding network of dislocations, originating at the point of collision. It appears that contact with a foreign particle creates dislocation sources in the crystal surface. As the crystal goes on growing, these sources, as a result of thermal stresses, give rise to more dislocations, which later act in their turn as new sources, and so on. The existence of dislocation sources of this type has only recently become evident. From the experiment referred to in the previous paragraph, in which the crystal was suddenly cooled by withdrawing it from the melt, it appears that surface sources of this nature do not occur in a crystal grown from a melt whose surface is clean.

---

[2]) The mechanism of this process is described e.g. by H. G. van Bueren, Philips tech. Rev. **15**, 255, 1953.

[3]) P. Penning, Philips Res. Repts. **13**, 79, 1958. See also P. Penning, The generation of dislocations by thermal stresses, Philips tech. Rev. **19**, 357-364, 1957/58.

[4]) The same was found by Dash for silicon: W. C. Dash, J. appl. Phys. **30**, 459, 1959.

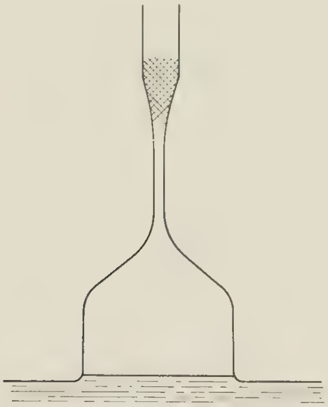

Fig. 2. In the necked portion of the crystal the dislocations as they grow with the crystal are bound to intersect the surface, where they must necessarily end; new dislocations cannot form because the thermal stresses are too small. In the lower portion, of large diameter, the thermal stresses are considerable, but now they create no dislocations because there are no longer any dislocation sources present.

Evidence for the absence of dislocations

In order to demonstrate that a crystal is free of dislocations, reliable methods are needed for detecting the presence of dislocations. One of the best available methods is that based on etch pits. If a germanium crystal is cut parallel to a (111) plane and etched with a suitable agent [5]), it is found to dissolve quicker at places where a dislocation intersects the surface than elsewhere, so that after some time "etch pits" form at these places. This phenomenon is attributed to the fact that the crystal lattice around the dislocation is deformed and thus possesses at such locations a higher energy per unit volume. The etch pits can easily be observed and counted under a microscope (*figs. 3* and *4*).

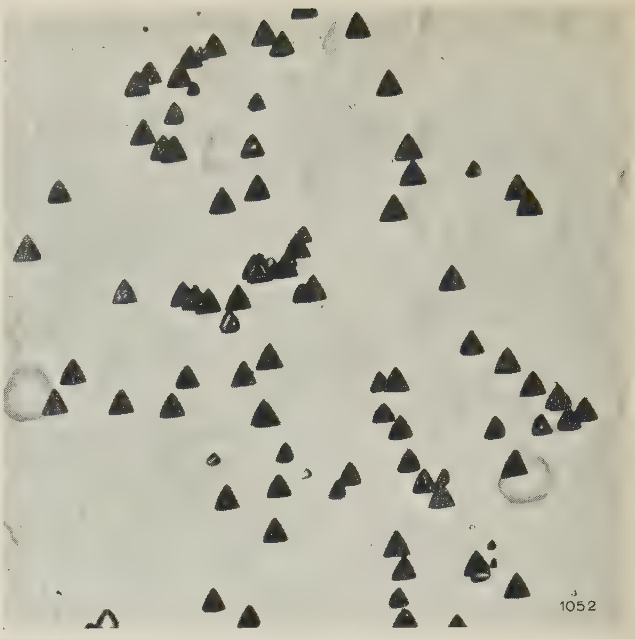

Fig. 3. If a germanium crystal is cut parallel to a (111) plane and etched with a suitable agent, the crystal dissolves quicker at the places where dislocations intersect the crystal surface then elsewhere. Each resultant etch pit corresponds to a dislocation. The sides of the triangular periphery of an etch pit are lines of intersection of the other (111) planes with the crystal surface. (Magnification 100 times.)

This etching procedure is simple to use and has proved very reliable. By various methods it has been shown that in Ge, at least, all dislocations are

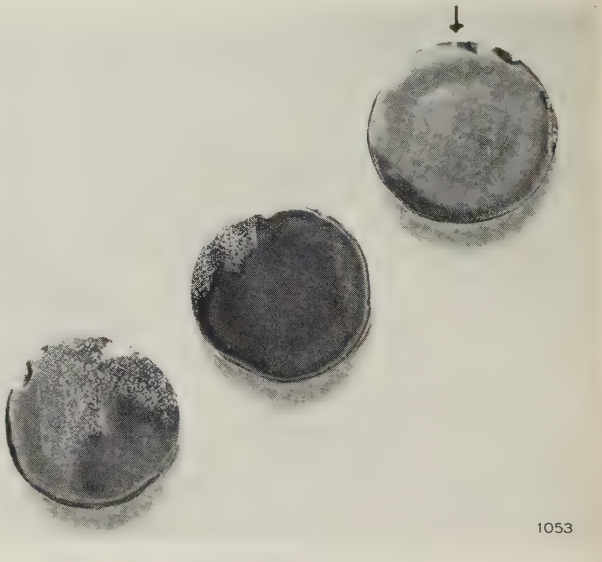

Fig. 4. Etched surface of three discs cut from an originally dislocation-free germanium crystal which, during the pulling process, came into contact with a piece of graphite on the melt. The disc on the right was cut at the point of collision; the two others were cut successively 5 mm further in the subsequently solidified part of the crystal. At the point of collision (see arrow) dislocation sources were evidently produced, from which stems a growing network of dislocations.

---

[5]) Use can be made of the etchant described by E. Billig, Proc. Roy. Soc. **A 229**, 346, 1955, or of the etchant known as CP4, the composition of which is described in the article by Vogel et al. under footnote [6]).

shown up in this way [6]). Various experiments carried out by us have also led to the same conclusion: the dislocation densities determined by the etching method on germanium crystals were compared with the results of two other methods. The first is based on the anomalous transmission of X-rays — an effect found only in perfect or nearly perfect crystals — and the second consists of determining the rate at which copper precipitates in a germanium crystal supersaturated with copper; this precipitation rate is governed solely by the dislocation density and the temperature (see appendix). At all the dislocation densities measurable by these methods — the lower limit of detection in our case was about 50 cm^{-2} for both methods, the upper limit for the X-ray method is some thousands of cm^{-2} — the results showed excellent agreement with those of the etch-pit method.

After etching, nearly all the germanium crystals grown by the method described above were found to be entirely free of etch pits (*fig. 5*). For this reason we believe we may conclude that these crystals are free of dislocations. In the few that were not dislocation-free, the dislocation density is several times 10^3 cm^{-2}. The negative result in these cases is most probably due to a trivial cause, such as the presence of an overlooked piece of solid matter on the surface of the melt.

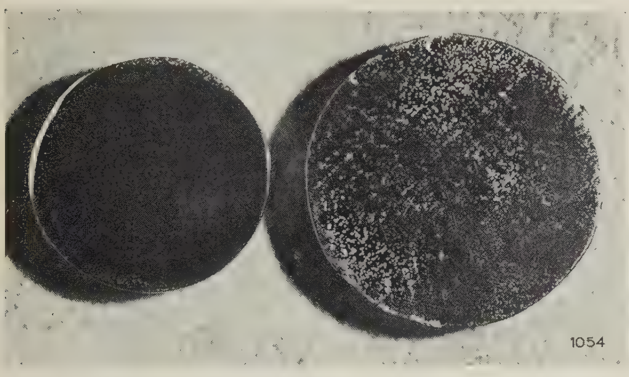

Fig. 5. Etched surface of a germanium crystal pulled by the method described (left) and of a crystal made without special precautions during the pulling process. The left crystal shows no etch pits, and this warrants the conclusion that it contains no dislocations.

It might be asked whether the above conclusion is indeed justified, and whether it is not conceivable that the crystals appear to be dislocation-free only because the dislocations present do not happen to intersect the etched surface. The answer is that the chance of this happening in the crystals made by the method described is exceptionally small. As already noted, the thermal stresses in a crystal of normal diameter (1 to 3 cm) are considerable. As a result, the dislocation density, unless it is zero, will always be high (10^3 to 10^4 cm^{-2}) even though there was originally only one source. The chance that no single one of these dislocations will intersect the etched surface may be considered to be zero — indeed, even at a dislocation density of, say, 10 cm^{-2}, this chance would be negligible. If not a single etch pit is found in a crystal, it is therefore highly probable that the crystal is entirely free of dislocations.

In passing it may be remarked that it follows from this reasoning that, in order to demonstrate the absence of dislocations in these crystals, it is not necessary that the detection method should detect every dislocation. In practice the etch-pit method is commonly used, not so much because of its sensitivity but because it is simple.

Various investigations have shown that dislocation-free germanium crystals are not perfect. During etching, most samples do not dissolve at a uniform rate at all parts of a cross-section (see fig. 4). Moreover, the anomalous transmission of X-rays through bent crystals is found to depend strongly on position. These effects indicate that the material is not homogeneous. This is probably attributable to a non-uniform distribution of the vacancies (or vacancy agglomerates) with which these crystals are in fact supersaturated. Since there are no dislocations that can function as sinks (see appendix) the vacancies in dislocation-free crystals must diffuse all the way to the crystal surface in order to disappear. Large numbers of vacancies have insufficient opportunity to do so during the cooling of the crystal and are therefore frozen-in.

Appendix: Determining the dislocation density from the anomalous transmission of X-rays and from the precipitation rate of copper

Anomalous transmission of X-rays [7])

The transmission of X-rays incident at the Bragg angle on a perfect crystal, i.e. at the angle Θ that satisfies the Bragg law, can be described by resolving the wave phenomenon in the crystal into two components (*fig. 6*). In a direction parallel to the lattice planes that reflects the X-ray beam, both components have the character of a travelling wave; in the direction perpendicular thereto they behave like a standing wave having a period equal to the lattice spacing d. Upon emerging from the crystal the two components split into a transmitted and a diffracted beam. The amplitude pattern of the one component (A) is now such that the minima coincide with the atomic planes and the maxima fall in between. There is therefore virtually no absorption of this component. On the other hand the maxima of the other component (B) coincide with the atomic planes, so that this component is strongly absorbed.

---

[6]) See F. L. Vogel, W. G. Pfann, H. E. Corey and E. E. Thomas, Phys. Rev. **90**, 489, 1953 and W. C. Dash, J. appl. Phys. **27**, 1193, 1956.

[7]) See L. P. Hunter, J. appl. Phys. **30**, 874, 1959, where references are given to earlier literature.

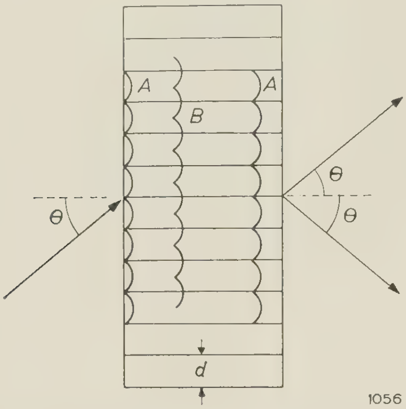

Fig. 6. Illustrating the anomalous transmission of X-rays incident at the Bragg angle on a group of parallel lattice planes of a nearly perfect crystal.

If the crystal is not perfect, e.g. owing to the presence of dislocations, then the first component, too, can suffer a degree of absorption. It is found that the intensity of the transmitted and of the diffracted beam both decrease markedly as the dislocation density of the crystal increases. The lowest dislocation density that could be demonstrated in this way with the apparatus used was about 50 cm^{-2}; it should certainly be possible, however, to lower this limit.

Calculating the dislocation density from the precipitation rate of copper

The possibility of determining the dislocation density in germanium by measuring the precipitation rate of copper is based on the interaction between dislocations and vacancies on the one hand and between the dissolved copper atoms and vacancies in the germanium on the other [8].

Copper atoms can be found in two kinds of site in the germanium lattice; they can replace a germanium atom in the lattice (substitution) or they may occupy an interstitial site. We shall denote atoms of the first kind by Cu_s, and atoms of the second kind by Cu_i. The concentrations of these atoms are not independent of each other; there exists an equilibrium $Cu_s \rightleftarrows Cu_i + V$. In this equation V represents the vacancy produced when a substitutional copper atom abandons its lattice site for an interstitial site. The substitutional copper atoms are strongly bound to their sites (the diffusion constant is approximately 10^{-11} cm^2/s) as are the vacancies. The interstitial atoms, on the other hand, are extremely mobile (diffusion constant approximately 10^{-5} cm^2/s).

If we now saturate a germanium crystal at 750 °C with copper and then, after cooling, we raise the crystal to a temperature of 500 °C, the crystal at the latter temperature will be about 1000-fold supersaturated with substitutional copper atoms. (The solubility of substitutional copper at 750 °C and 500 °C is respectively 10^{16} and 10^{13} atoms per cm^3. The concentration of the interstitial atoms can be disregarded, since, owing to the high mobility of the interstitial atoms, it never differs significantly from the equilibrium value.) The excess substitutional copper atoms can only disappear from the crystal by first becoming interstitial. Since the vacancies thereby produced can diffuse but slowly to a site capable of functioning as a "sink" for vacancies — such as a dislocation, or the surface of the crystal — a state of quasi-equilibrium arises in which the ratio between the concentrations of the substitutional copper atoms and the vacancies is constant. The rate at which the excess copper disappears, and thus at which the solution changes from a supersaturated to the normal saturated condition, is therefore determined by the rate at which the vacancies can be removed. The latter rate depends in its turn on the number of sinks present, i.e. on the dislocation density.

Conversely, then, one can determine the dislocation density by measuring at a certain temperature T (in our case 500 °C) the time constant τ of the exponential time-variation of the substitutional Cu concentration towards its equilibrium value. In practice this is done by examining the way in which the resistivity of the crystal varies with time during the period in which the crystal is held at the temperature T. Clearly, the value of τ thus found also depends on this temperature.

It is found that the product of τ and the dislocation density N has a constant value at a given temperature. The relation between τ and $1/T$, as found experimentally by Tweet [8], is shown in *fig. 7*. It is seen from this figure that at 500 °C the product $\tau \times N$ has roughly the value 10^9. Thus, if we find at a temperature of 500 °C a τ value of, say, 10^4, we may conclude that the dislocation density is approximately 10^5 cm^{-2}. The smallest density at which the presence of dislocations can be detected by this method is about 50 cm^{-2}, as in the previous case.

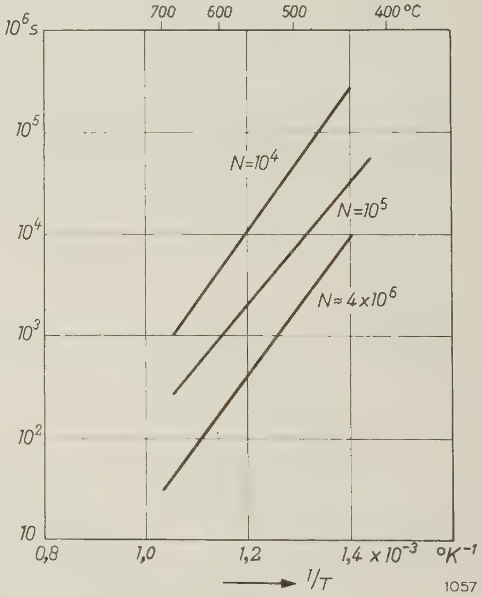

Fig. 7. The time constant τ of the rate of precipitation of copper in supersaturated germanium, plotted as a function of the reciprocal of the absolute temperature T, for three germanium crystals of differing dislocation densities N (cm^{-2}). (After Tweet [8].)

Finally, a word about the way in which a dislocation can function as a sink for vacancies. It is known that an edge dislocation may be thought of as arising from the insertion of an extra atomic plane, the edge of which is located inside the crystal. Now it is very well possible that an atom at the edge of this plane may break away and occupy the site of a neighbouring vacancy site. This is particularly the case if the dislocation contains a jog: the latter then moves along the dislocation by one lattice site (*fig. 8*). A vacancy moves along a dislocation relatively fast, and the time needed to reach such a jog is equal, to a first approximation, to the time needed for a vacancy to diffuse to the dislocation.

---

[8] A. G. Tweet, Phys. Rev. **106**, 221, 1957, and P. Penning, Philips Res. Repts. **13**, 17, 1958.

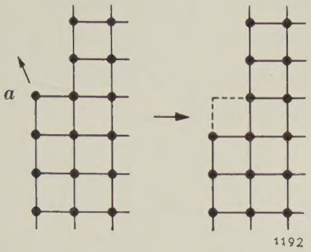

Fig. 8. An edge dislocation with a "jog" in it readily serves as a sink for vacancies. The drawing shows a part of the extra atomic half-plane of the dislocation containing a jog (left). If the atom *a* breaks away to occupy the site of a neighbouring vacancy, the jog shifts laterally along the dislocation by one lattice site as shown on the right.

Summary. Dislocation-free germanium crystals can be produced by the pulling method if the diameter of the crystal grown from the seed is initially reduced to 1 or 2 mm. This diameter is maintained over a length of about 20 mm, after which it is gradually raised to the desired value. In the thin neck of crystal thus produced the dislocations present tend to intersect the surface somewhere, where they end; thermal stresses are too small to generate fresh dislocations. The thermal stresses generally increase as the crystal diameter is increased but no dislocations are created because of the absence of sources. However, should a piece of solid material floating on the melt come into contact with the growing crystal, dislocation sources are produced in the surface. Freedom from dislocations is demonstrated by the etch-pit method. Dislocation-free single crystals still contain point defects.

ABSTRACTS OF RECENT SCIENTIFIC PUBLICATIONS BY THE STAFF OF N.V. PHILIPS' GLOEILAMPENFABRIEKEN

Reprints of these papers not marked with an asterisk * can be obtained free of charge upon application to Philips Electrical Ltd., Century House, Shaftesbury Avenue, London W.C. 2.

2706: D. J. Kroon and C. van de Stolpe: Positions of protons in aluminium hydroxides derived from proton magnetic resonance (Nature **183,** 944-945, 1959, No. 4666).

Note concerning the determination of proton positions in hydrargillite (γ-Al(OH)$_3$), boehmite (γ-AlOOH) and bayerite (α-Al(OH)$_3$). See also Philips tech. Rev. **21,** 290, 1959/60 (No. 10).

2707: F. K. Lotgering: Topotactical reactions with ferrimagnetic oxides having hexagonal crystal structures, I (J. inorg. nucl. Chem. **9,** 113-123, 1959, No. 2).

A new method is described for the preparation of polycrystalline materials with oriented crystals by reaction of the oriented grains of a strongly anisotropic ferrimagnetic with non-oriented grains of usually non-magnetic components. Using this type of reaction, for which the name "topotactical (or "topotaxial") reaction" is proposed, oriented samples of $Ba_3Co_\delta Zn_{2-\delta}Fe_{24}O_{41}$, $BaCo_\delta Zn_{2-\delta}Fe_{16}O_{27}$ and $BaCo_\delta Ti_\delta Fe_{12-2\delta}O_{19}$, which have related hexagonal crystal structures, have been prepared as well as some ferrites having the cubic spinel structures. See also Philips tech. Rev. **20,** 354, 1958/59.

2708: H. A. Klasens: The temperature dependence of the fluorescence of photoconductors (Phys. Chem. Solids **9,** 185-197, 1959, No. 3/4).

In a previous paper (No. **2650**), the effects of exciting intensity on the behaviour of a fluorescent photoconductor were discussed, using a two-state model with one level near the conduction band and occupied by an electron in the dark and one state near the conduction band and not occupied in the dark. In the present paper the effect of temperature in the stationary state for such a model is discussed. The lower level is assumed to be an activator level giving rise to a fluorescent transition, whereas the other level is attributed to a killer centre. The phosphor is excited with long wavelengths bringing electrons from the activator level to the conduction band.

It is shown that the nature of the temperature-dependence curve can be strongly affected by the capture cross-sections for electrons and holes of the two centres. A plot of log $\{(I_0/I) - 1\}$ versus T^{-1} will in general not produce straight lines as in the case of non-photoconducting phosphors, and no conclusions can be drawn from such a plot regarding the positions of the impurity levels.

The best way to determine the position of the activator level is to excite the phosphor at high intensities. A plot of log $\{(I_0/I)^{\frac{1}{2}} - (I/I_0)^{\frac{1}{2}}\}$ versus T^{-1} will then have a slope corresponding to the thermal-energy difference between the activator level and the top of the highest occupied band.

2709: J. van Dijk and H. D. Moed: Synthesis of β-phenylethylamine derivatives, VI. Stereoisomers of 1-(4′-hydroxyphenyl)-2-(1″-methyl-2″-phenoxyethylamino) propanol-1 (Rec. Trav. chim. Pays-Bas **78,** 22-42, 1959, No. 1).

The synthesis is described of the four pairs of enantiomeric modifications of

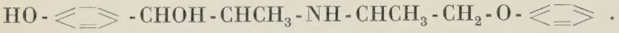

The stereochemical structures have been correlated with those of erythro- and threo-ephedrine. Conformation analysis has been used to explain the configuration of the amino-alcohols formed.

2710: H. M. Jongerius, J. L. van Koeveringe and H. J. Oskam: Argon-xenon bands (Physica **25,** 406-408, 1959, No. 5).

Note reporting on the spectrum of a 50-50 mixture of argon-xenon. The edge of the negative glow is bright green, and contains two bands that are absent from the spectra of both argon and xenon.

2711: G. Meijer: The spectral dependence of flowering and elongation (Thesis, Utrecht, 8 June 1959).

Experiments with *Salvia occidentalis* (SDP) and *Hyoscyamus* niger (LDP) demonstrated that at least two photoperiodic reactions are involved in the process leading to a long-day effect. The main-light-period reaction is more sensitive to near infrared and blue light than to red or green light. The effect of near infrared and blue light can be antagonized by red light. The night-break reaction, promoted by red light, is nullified by a relatively short exposure to near infrared or blue light.

Experiments with various plant species on the elongation of internodes have shown that at relatively low intensities red light is more inhibitive than blue light. At relatively high intensities blue light is the most inhibiting spectral region. The inhibiting effect of red light on the elongation of hypocotyls of light-grown gherkin seedlings is antagonized by a subsequent exposure to near infrared or blue light. The inhibiting effect of red light on the hypocotyl of dark-grown gherkin seedlings is much more pronounced when the seedlings are pre-irradiated with white or blue light.

2712: J. Brug, R. J. E. Esser and G. B. Paerels: The enzymic cleavage of N-acetylneuraminic acid (Biochim. biophys. Acta **33,** 241-242, 1959, No. 1).

Under the influence of an enzyme in a filtrate of *Vibrio cholerae,* both natural and synthetic N-acetylneuraminic acid is broken down to N-acetyl-d-mannosamine and not to N-acetyl-d-glucosamine, as hitherto supposed. Under the experimental conditions no epimerization of the N-acetylamino sugars occurs. This result therefore forms a confirmation of the structure of N-acetylneuraminic acid proposed by Comb and Roseman.

2713: A. J. W. Duijvestijn: On the transition from superconducting to normal phase, accounting for latent heat and eddy currents (IBM J. Res. Devel. **3,** 132-139, 1959, No. 2).

A rigorous solution is given for the superconducting transition of a semi-infinite slab held at a point below the critical temperature T_c when a constant magnetic field above the critical value H_{0c} is applied. The solution accounts for both the absorption of latent heat and the dissipation of eddy-current heat during the transition. A numerical example is calculated for the case of constants close to those of tantalum.

2714: P. Jongenburger and C. W. Berghout: A null coil magnetometer (Appl. sci. Res. **B 7,** 366-378, 1959, No. 5).

A magnetometer has been developed in which the saturation-magnetization of small samples of ferromagnetic materials can be measured. The sample, which is situated at the centre of a small coil, is placed in an inhomogeneous magnetic field. The current through the coil is adjusted to such a value that the forces on coil and sample balance each other. Under certain conditions the magnetic moment of the sample then equals the magnetic moment of the coil; these conditions are discussed. The method is suitable for use in ordinary laboratory magnets and in solenoids, also at low temperatures. With a second version of this magnetometer it is possible to measure para- and even diamagnetism.

2715: W. F. Schalkwijk: A simplified regenerator theory (Trans. ASME **A 81,** 142-150, 1959, No. 2).

Most regenerators encountered in practice have simple linear or exponential temperature fields in their central parts. This leads to the possibility of a simplified representation of the regenerator efficiency with sufficient accuracy for all practical cases. In the important “symmetrical” case, in which the parameters have the same value in both directions of gas flow, the efficiency can be represented by a single curve. This case is treated extensively in this paper. The results for the general case are given in an appendix. Here also a reduction is achieved of the number of parameters needed to represent the efficiency.

2716: J. F. Schouten: De beoordeling van perceptieve en selectieve belasting (T. soc. Geneesk. **37**, 393-395, 1959, No. 10). (Appraisement of perceptive and selective tasks; in Dutch.)

In industry, personnel are less and less used as instruments of mechanical energy and more and more as instruments of selection. Analysis of human selective ability is therefore desirable. It is necessary to study this ability in relation to working tempo, education and fatigue, both during the learning period and during the stabilized work-process. An example of a test to facilitate this analysis, developed in the Institute for Perception Research (Eindhoven), is described. The test is concerned with the fitting of pegs in holes, and gives some insight into the general way in which such investigations can be pursued.

2717: O. Reifenschweiler: A suitable tritium carrier for gas-discharge tubes (Proc. 2nd United Nations int. Conf. on the peaceful uses of atomic energy, Geneva 1-13 Sept. 1958, Vol. 19, pp. 360-362).

Tritium is a radioactive substance with attractive properties for use as an ionizing agent to facilitate the triggering of gas discharges. In order to introduce the tritium into the discharge tube the author has devised a method in which the tritium is absorbed in titanium powder. A suspension of the powder in a binder medium is painted with a brush on a suitable surface. To preclude that the electrons emitted are absorbed by the powder itself the particles of Ti must be extremely small. The manner of preparing such a fine powder (particle size $\sim$ 200 Å) is described.

2718: J. L. Meijering and M. L. Verheijke: Oxidation kinetics in the case of aging oxide films (Acta metallurgica **7**, 331-338, 1959, No. 5).

The cubic relationship found by Hauffe and Kofstad for the rate of oxidation of Cu_2O in the 800-1000 °C range is confirmed, and also the abnormally low temperature coefficient of the rate constant. Special experiments show that aging effects in the CuO layer must be responsible for this behaviour. Calculations of the oxidation kinetics are given for the case when the permeability (or its reciprocal) of the oxide formed changes exponentially with age.

2719: K. W. van Gelder: Fabricagebeheersing, II. Het aanhouden van toleranties (Sigma **5**, 33-38, 1959, No. 2). (Process control, II. The meeting of tolerances; in Dutch.)

Continuation of No. **2702.** This second article deals with problems associated with the meeting of the specified tolerances, both as regards the production line itself and the inspection. In conclusion an attempt is made to set up a usable relation between quality and production costs.

2720: J. J. Arlman and H. N. L. Hoevenaar: Een niveaudetector voor de praktijk (Ingenieur **71**, Ch. 8-Ch. 9, 1959, No. 19). (A practical level detector; in Dutch).

For the determination of the liquid level in closed cylinders a simple apparatus was designed, consisting of a radioactive Cs-137 source holder and a transistorized monitor to measure the gamma radiation. This instrument provides a new method for a quick control of CO_2 fire protection installations on shipboard, which means that the time-wasting demounting, weighing and remounting of the cylinders is done away with. The simple principle permits of many applications by a mere adjustment of the source holder to the special situation considered.

2721: B. Combée and P. J. M. Botden: De mogelijkheden van teleröntgendiagnostiek, zoals bedreven in Jean Talon Hospital, Montreal (J. belge Radiol. **42**, 79-86, 1959, No. 1). (The possibilities of X-ray tele-diagnostics as practiced at the Jean Talòn Hospital, Montreal; in Dutch.)

The X-ray image intensifier, together with a simply-operated television camera, makes X-ray diagnostics possible in daylight. The shielding of the operator is no longer a problem and the dose received by the patient is reduced. The installation in the Jean Talon Hospital in Montreal is described.

2722: W. Verweij and M. H. A. van de Weijer: New sodium lamps (Commission internationale de l'éclairage, 14th session, Brussels 1959).

A new design of sodium lamp is described adopting a single evacuated outer bulb around the discharge tube. The physical background to the dimensioning of these lamps is discussed. Despite its simple construction, which is considerably lighter than its predecessors with their separate vacuum jackets, a satisfactory thermal stability is ensured by choosing the right dimensions and rare gas filling. Various features combine to give a good life performance. The use of a non-discolouring glass and depressions in the discharge tube wall which ensure a uniform distribution of the sodium and at the same time prevent the formation of sodium mirrors, improve the lumen maintenance of the new lamp as compared with the older types. Ignition voltage trouble due to rare-gas disappearance is avoided by the selection of a suitable rare gas filling. In addition to these new lamps, which are interchangeable with the older types of 45, 60, 85, and 140 W lamps using separate vacuum jackets, some experimental models for a loading of approx. 250 W are discussed.

A 12: A. Rabenau and P. Eckerlin: Zur Frage der Existenz von Verbindungen mit K_2NiF_4-Struktur (Z. anorg. allgem. Chem. **303**, 103-104, 1960, No. 1/2). (Concerning the existence of compounds with K_2NiF_4 structure; in German.)

Remarks on a paper by Wagner and Binder concerning the existence of compounds with K_2NiF_4 structure, which does not depend on the existence of a corresponding cubic perovskite.

A 13: G. Arlt: Halleffekt-Vierpole mit hohem Wirkungsgrad (Solid-State Electronics **1**, 75-84, 1960, No. 1). (High-efficiency Hall-effect fourpoles; in German.)

The upper efficiency limit of the Hall gyrator with four electrodes is 0.17. To enlarge the efficiency one has to solder more than one polarizing-current circuit and Hall circuit to the same Hall specimen. This holds for all types of Hall devices such as generator, gyrator, isolator, circulator, etc. Methods are given for the calculation of the highest possible efficiency and other interesting properties. Gyrators and isolators are proposed for audio, high and ultra-high frequency applications. Series-parallel connexion of gyrator and transformator yields a low-loss uniline.

A 14: A. Klopfer and W. Ermrich: Eigenschaften von Getter-Ionenpumpen (Vakuum-Technik **8**, 162-167, 1959, No. 6). (Properties of getter ion pumps; in German.)

The characteristic properties of getter ion pumps are reviewed, e.g. pumping capacity and pumping speed. In order to obtain low pressures it is essential to have information available on various gas-getter reactions and on desorption processes. Such mechanisms determine the ultimate pressure and the efficiency of getter ion pumps.

A 15: I. Maak and A. Rabenau: Zur Kenntnis des LiP (Angew. Chemie **72**, 268, 1960, No. 7/8). (On the compound LiP; in German.)

Note reporting three methods of preparing LiP.

A 16: P. Eckerlin, C. Langereis, I. Maak and A. Rabenau: Über $LiPN_2$ (Angew. Chemie **72**, 268, 1960, No. 7/8). (On the compound $LiPN_2$; in German.)

Note on the preparation, chemical behaviour and crystal structure of $LiPN_2$.

A 17: S. Scholz: Untersuchungen zum Einfluß des Peltier-Effektes auf Widerstands-Schweißungen (Z. angew. Physik **12**, 111-117, 1960, No. 3). (Investigation into the influence of the Peltier effect on resistance welding; in German.)

In resistance welding of two different metals the Peltier effect gives rise to welds of varying depth according to the direction of the current pulses. The magnitude of the effect is estimated: for the couple gold-palladium the Peltier heat is about 10% of the electrical energy used for the welding. Measurements confirm this result. (See also Philips tech. Rev. **20**, 188-192, 1958/59.)

A 18: A. Rabenau, A. Stegherr and P. Eckerlin: Untersuchungen im System Tellur-Thallium (Z. Metallkunde **51**, 295-299, 1960, No. 5). (Investigation of the system tellurium-thallium; in German.)

Investigations of the system tellurium-thallium were made by thermal analysis, metallographical and X-ray examination. Besides the congruently melting γ-phase and the peritectic compound TlTe a new peritectic compound with the composition Tl_2Te_3 was found. The composition range of the γ-phase could be fixed. The crystallographic data of the intermediate phases were determined.